J. Fluid Mech. (2007), *vol.* 576, *pp.* 235–264. © 2007 Cambridge University Press
doi:10.1017/S0022112006004484 Printed in the United Kingdom

Scattering of surface gravity waves by bottom topography with a current

FABRICE ARDHUIN AND RUDY MAGNE

Centre Militaire d'Océanographie, Service Hydrographique et Océanographique de la Marine, 29275 Brest, France
ardhuin@shom.fr

(Received 7 October 2005 and in revised form 28 September 2006)

A theory is presented that describes the scattering of random surface gravity waves by small-amplitude topography, with horizontal scales of the order of the wavelength, in the presence of an irrotational and almost uniform current. A perturbation expansion of the wave action to order η^2 yields an evolution equation for the wave action spectrum, where $\eta = \max(h)/H$ is the small-scale bottom amplitude normalized by the mean water depth. Spectral wave evolution is proportional to the bottom elevation variance at the resonant wavenumbers, representing a Bragg scattering approximation. With a current, scattering results from a direct effect of the bottom topography, and an indirect effect of the bottom through the modulations of the surface current and mean surface elevation. For Froude numbers of the order of 0.6 or less, the bottom topography effects dominate. For all Froude numbers, the reflection coefficients for the wave amplitudes that are inferred from the wave action source term are asymptotically identical, as η goes to zero, to previous theoretical results for monochromatic waves propagating in one dimension over sinusoidal bars. In particular, the frequency of the most reflected wave components is shifted by the current, and wave action conservation results in amplified reflected wave energies for following currents. Application of the theory to waves over current-generated sandwaves suggests that forward scattering can be significant, resulting in a broadening of the directional wave spectrum, while back-scattering should be generally weaker.

1. Introduction

Following laboratory observations by Heathershaw (1982), a considerable body of knowledge has been accumulated on the scattering of small-amplitude surface gravity waves by periodic bottom topography. An asymptotic theory for small bottom amplitudes, that reproduces the observed scattering of monochromatic waves over a few sinusoidal bars, was put forward by Mei (1985), leading to practical phase-resolving equations that may be used to model this phenomenon for more general bottom shapes (Kirby 1986). For sinusoidal bottoms of wavenumber l, Mei (1985) proposed an approximate analytical solution. In two dimensions (one horizontal and the vertical) this solution yields simple expressions for the wave-amplitude reflection coefficient R, as a function of the mismatch between the wavenumber of the surface waves k and the resonant value $l/2$, for which R is maximum due to Bragg resonance. Beyond a cutoff value of that mismatch, it was found that the incident and reflected wave amplitudes oscillate in space instead of decreasing monotonically from the

https://doi.org/10.1017/S0022112006004484 Published online by Cambridge University Press

incident region. Guazzelli, Rey & Belzons (1992) have shown that higher-order theories are necessary to represent the subharmonic resonance observed over a bottom that is a superposition of two sinusoidal components of different wavelengths. Such subharmonic resonance was found to have as large an effect as the lowest-order resonance for bottom amplitudes of only 25 % of the water depth, due to a stronger reflection for longer waves in their case.

In three dimensions (in which case propagation is along the two horizontal dimensions), many wave components may interact as the Bragg resonance condition becomes $\boldsymbol{k} = \boldsymbol{l} + \boldsymbol{k}'$ and $\omega = \omega'$, with ω and ω' the wave radian frequencies corresponding to the wavenumber vectors $\boldsymbol{k}$ and $\boldsymbol{k}'$. Amplitude evolution equations such as derived by Mei (1985) are prohibitively expensive for investigating the propagation of random waves over distances larger than about 100 wavelengths, and the details of the bottom are typically not available over large areas. A consistent phase-averaged wave action evolution equation is also necessary for the investigation of the long waves associated with short wave groups (Hara & Mei 1987). The large-scale behaviour of the wave field may, rather, be represented by the evolution of the wave action spectrum assuming random phases. Such an approach had been proposed by Hasselmann (1966) and Elter & Molyneux (1972) for the calculation of wind-wave and tsunami propagation, respectively. An appropriate theory for the evolution of the wave spectrum can be obtained from a solvability condition, a method similar to that of Mei (1985) and Kirby (1988), but applied to the action spectral densities instead of the amplitudes of monochromatic waves. In the absence of currents, the correct form of that equation was first obtained by Ardhuin & Herbers (2002, hereinafter referred to as AH) using a two-scales approach. They decomposed the water depth $H - h$ into a slowly varying depth H, that causes shoaling and refraction, and a rapidly varying perturbation h with zero mean, that causes scattering. The resulting evolution equation for the wave spectrum is formally similar to general transport equations for waves in random media (e.g. Ryzhik, Papanicolaou & Keller 1996). This equation predicts a scattering that was shown to be consistent with the dramatic increase of the directional width of the wave spectra, observed on the North Carolina continental shelf (Ardhuin *et al.* 2003*a*, *b*).

The scattering theory of AH is similar to Bragg scattering approximations for acoustic and electromagnetic waves. These approximations are usually obtained by the small-perturbation method, valid in the limit of small $k\max(h)$ where k is the wavenumber of the propagating waves (Rayleigh 1896, see Elfouhaily & Guérin 2004 for a review of this and other approximations). Since there is no scattering for $kH \gg 1$, as the waves are not affected by the bottom, $k\max(h)$ may be replaced by $\eta = \max(h)/H$. For $\eta \ll 1$, the scattering strength is thus entirely determined by the bottom elevation variance spectrum at the bottom scales resonant with the incident waves. This result was first established by Kreisel (1949) for normal incidence over a topography uniform in one dimension, and extended by Miles (1981) to oblique incidence.

Consistent with Kreisel's (1949) result, Magne *et al.* (2005*a*, hereinafter referred to as MAHR) showed that AH's theory gives the same damping of incident waves as the Green function solution of Pihl, Mei & Hancock (2002), applied to any two-dimensional topography, random or not. Investigating the applicability limits of the scattering term of AH, MAHR also performed numerical calculations, comparing AH's theory to the accurate matched-boundary model of Rey (1992) that uses a decomposition of the bottom into a series of steps, including evanescent modes. The numerical results show that AH's theory is generally limited by the relative bottom

https://doi.org/10.1017/S0022112006004484 Published online by Cambridge University Press

amplitude $\eta = \max(h)/H$ rather than the bottom slope. In particular, AH's theory predicts accurate reflections, with a relative error of order η, even for isolated steps that have an infinite slope.

Given these results, Mei's (1985) solutions should yield the same reflection coefficient as AH's theory in the limit of small bottom amplitudes. Yet, AH predict that the wave amplitude in two dimensions would decay monotonically, which is not compatible with the oscillatory nature of Mei's theory for large detunings from resonance, a prediction verified in the laboratory by Hara (1996, see also Hara & Mei 1987). Further, outside the surf zone and the associated multiple bar systems, the application of AH's theory is most relevant in areas where the bottom topography changes on the scale of the wavelengths of swells. Over sand, this often corresponds to the presence of sandwaves. These sandwaves are generated by currents, and particularly by tidal currents (e.g. Dalrymple, Knight & Lambiase 1978; Idier, Erhold & Garlan 2002). It is thus logical to include the effects of currents in any theory for wave scattering over a random bottom. Kirby (1988) developed such a theory for monochromatic waves over a sinusoidal bottom and a slowly varying mean current, extending Mei's (1985) work. The geometry of the resonant wavenumbers is modified in that case, with incident and reflected waves having the same absolute frequency, but different wavenumber magnitudes. Kirby (1988) also considered the short-scale fluctuations of the current, due to the sinusoidal bottom, that may be interpreted as an extra source of scattering, identical to the scattering of gravity and gravity–capillary waves over irrotational current fluctuations studied by Watson & West (1975) and Bal & Chou (2002). It should be noted that a more general theory for deep-water waves over any current was given by Rayevskiy (1983) and Fabrikant & Raevsky (1994).

The present paper thus addresses the following two questions: What is the difference between Mei's (1985) and AH's theories? What is the effect of a current? An extension of AH's theory for surface gravity wave scattering in the presence of irrotational currents with uniform mean velocities is provided in § 2, and the differences between this theory and those of Mei (1985) and Kirby (1988) are discussed in § 3. The more general case of short-crested waves over a random topography in the presence of a current is investigated in § 4, with a brief description of expected oceanographic effects. Conclusions and perspectives follow in § 5.

2. Theory

2.1. *General formulation*

The evolution of the action spectrum due to wave–bottom scattering is derived following the method of AH, now including the effect of a nearly uniform mean current. The method is similar to that of Kirby (1988) with the difference that an equation for the spectral wave action is sought instead of one for the wave amplitudes. The only important terms in this type of calculation are the 'secular terms', i.e. the harmonic oscillator solutions for the wave potential forced at resonance, with an amplitude that grows unbounded in time. We shall thus obtain a rate of change of the action by imposing that the sum of all the secular terms be zero. The particularity of the random wave approach is also that we will consider all possible couplings between wave components, and not just two wave trains. With random waves, secularity is limited to a sub-space of the wavenumber plane that generally has a zero measure. But the near-resonant terms, once integrated across the resonant singularity, are the ones that provide the secular terms for random waves (see e.g. figure 5 of Annenkov & Shrira 2006). This integration assumes that the spectral properties

https://doi.org/10.1017/S0022112006004484 Published online by Cambridge University Press

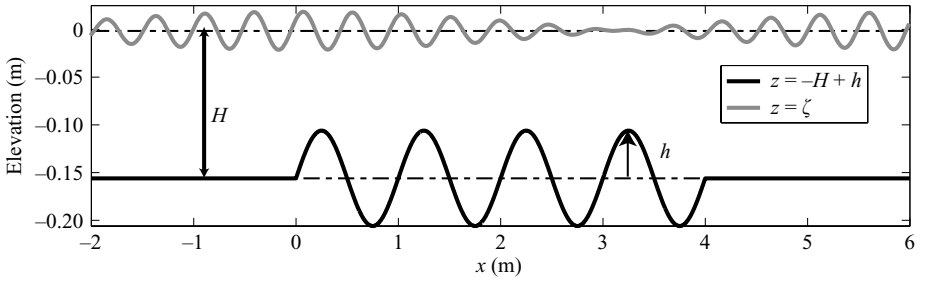


FIGURE 1. Definition sketch of the mean water depth H, and relative bottom elevation h, for one particular case of a sinusoidal bottom investigated in § 3.

are continuous, a real theoretical problem for nonlinear wave–wave interactions (e.g. Benney & Saffmann 1966; Onorato *et al.* 2004). Here we shall see that the only relevant condition is that the bottom spectrum be continuous, at least in one dimension. This is obviously satisfied by any real topography.

Assuming irrotational flow, we consider random waves propagating over an irregular bottom with a constant mean depth H and mean current $\boldsymbol{U}$, and a random topography $h(\boldsymbol{x})$, with $\boldsymbol{x}$ the horizontal position vector, so that the bottom elevation is given by $z=-H+h(\boldsymbol{x})$ where z is the elevation relative to the still water level (see figure 1). The current over bottom undulations h causes a stationary random small-scale mean surface elevation $\zeta_c(\boldsymbol{x})$ and current $(\boldsymbol{u}_c(\boldsymbol{x}, z), w_c(\boldsymbol{x}, z))$ derived from a potential ϕ_c. Extension to mean current and mean depth variations on a large scale follows from a standard two-scale approximation, already performed by Kirby (1988). This is not repeated here for brevity.

The maximum surface slope ε is assumed small ($\varepsilon^3 \ll \eta^2$) so that the bottom scattering contributions to the wave action to order η^2 are much larger than the resonant nonlinear four-wave interactions (Hasselmann 1962) which will therefore be neglected. For shallow-water waves ($kH \ll 1$) a stricter inequality is needed to prevent triad wave–wave interactions entering the action evolution equation at the same order as bottom scattering. Such interactions can also be added in the present calculation, providing an additional source of scattering with the known form due to quadratic or cubic nonlinearities. Since our purpose is the investigation of bottom-induced scattering, the combination with other scattering processes would add unnecessary complexity. We have therefore chosen ε small enough so that the waves are essentially linear.

The solution is obtained in a frame of reference moving with the mean current vector $\boldsymbol{U}$, which has the advantage of removing the largest convective terms since the mean current is zero in the moving frame of reference. The corresponding transformation of the horizontal coordinates is $\boldsymbol{x}'=\boldsymbol{x}+\boldsymbol{U}t$, where $\boldsymbol{x}$ and $\boldsymbol{x}'$ are the coordinates in the moving and fixed frames, respectively. As a result of this transformation, the bottom moves with an apparent velocity $-\boldsymbol{U}$, which leads to a modification of the bottom boundary condition for the velocity potential ϕ. The governing equations consist of Laplace's equation for ϕ, which includes both wave and current motions†, the bottom kinematic boundary conditions, and Bernoulli's equation with the free-surface kinematic boundary condition. Assuming that the atmospheric pressure is

† Because the frame of reference is moving with the mean current, the current fluctuations caused by the bottom and deriving from ϕ_c are included in ϕ.

https://doi.org/10.1017/S0022112006004484 Published online by Cambridge University Press

zero for simplicity, and neglecting surface tension, yields

$$\nabla^2\phi + \frac{\partial^2\phi}{\partial z^2} = 0 \quad \text{for} \quad -H + h \leqslant z \leqslant \zeta, \tag{2.1}$$

$$\frac{\partial\phi}{\partial z} = \frac{\partial h}{\partial t} + \nabla\phi\cdot\nabla h \quad \text{at} \quad z = -H + h, \tag{2.2}$$

$$\frac{\partial\phi}{\partial t} + g\zeta = -\frac{1}{2}|\nabla\phi|^2 - \frac{1}{2}\left(\frac{\partial\phi}{\partial z}\right)^2 + c(t) \quad \text{at} \quad z = \zeta. \tag{2.3}$$

$$\frac{\partial\phi}{\partial z} = \frac{\partial\zeta}{\partial t} + \nabla\phi\cdot\nabla\zeta \quad \text{at} \quad z = \zeta, \tag{2.4}$$

with $c(t)$ a function of time only, to be determined. The symbol ∇ represents the usual gradient operator restricted to the two horizontal dimensions. The last two equations may be combined to remove the linear part in ζ. Taking $\partial(2.3)/\partial t + g(2.4)$, yields

$$\frac{\partial^2\phi}{\partial t^2} + g\frac{\partial\phi}{\partial z} = g\nabla\phi\cdot\nabla\zeta - \frac{\partial\zeta}{\partial t}\frac{\partial^2\phi}{\partial z\partial t} - \left(1 + \frac{\partial\zeta}{\partial t}\frac{\partial}{\partial z}\right)\left[\nabla\phi\cdot\frac{\partial\nabla\phi}{\partial t} + \frac{\partial\phi}{\partial z}\frac{\partial^2\phi}{\partial t\partial z}\right] + c'(t), \quad \text{at} \quad z = \zeta. \tag{2.5}$$

Following Hasselmann (1962), we approximate h and ϕ with discrete sums over Fourier components, and take the limit to continuous integrals after deriving expressions for the evolution of the phase-averaged wave action. We look for a velocity potential solution in the form

$$\phi(\boldsymbol{x}, z, t) = \sum_{\boldsymbol{k},s} \widehat{\Phi}^s_{\boldsymbol{k}}(z, \gamma t)\mathrm{e}^{\mathrm{i}[\boldsymbol{k}\cdot\boldsymbol{x} - s\sigma t]} = \sum_{\boldsymbol{k},s} \Phi^s_{\boldsymbol{k}}(t)\frac{\cosh[k(z+H)]}{\cosh(kH)}\mathrm{e}^{\mathrm{i}\boldsymbol{k}\cdot\boldsymbol{x}} + \cdots, \tag{2.6}$$

where σ is the radian frequency in the moving frame, $\boldsymbol{k}$ is the surface wavenumber, with magnitude k, and s is a sign index equal to 1 or -1. In the moving frame of reference, $s = 1$ for wave components that propagate in the direction of the vector $\boldsymbol{k}$, and $s = -1$ for components that propagate in the opposite direction. Thus the radian frequency in the fixed frame is $\omega = \sigma + s\boldsymbol{k}\cdot\boldsymbol{U}$. The complex amplitudes $\widehat{\Phi}^s_{\boldsymbol{k}}$ are random and slowly modulated in time, with a slowness defined by the small parameter γ. As will be found below, here this evolution is due only to bottom scattering and γ will be found to be of order η, or η^2 if the wave–wave–bottom bispectrum is neglected. Because ϕ is real, $\widehat{\Phi}^s_{\boldsymbol{k}} = \overline{\widehat{\Phi}^{-s}_{-\boldsymbol{k}}}$, where the overbar denotes the complex conjugate. Thus the double decomposition made in (2.6) in wavenumber $\boldsymbol{k}$ and propagation direction $+$ or $-$ replaces a general decomposition in wavenumber and frequency that would be necessary if nonlinear dispersive effects were included. Here the frequency σ is always related to k via the linear dispersion relation.

In the alternative decomposition with amplitudes $\Phi^s_{\boldsymbol{k}}$ that contain the fast time variation, only the part of the solution that has the vertical structure of Airy waves has been given explicitly in (2.6). The other part, represented by '…', will be found to be negligible for small bottom amplitudes.

The bottom boundary condition and wave potential are expanded in powers of η:

$$\phi = \phi_0 + \phi_1 + \phi_2 + \cdots, \tag{2.7}$$

where each term ϕ_i is of order η^i. The boundary conditions (2.5) and (2.2) are expressed at $z = 0$ and $z = -H$, respectively, using Taylor series of ϕ about $z = -H$ and $z = 0$.

https://doi.org/10.1017/S0022112006004484 Published online by Cambridge University Press

Unless stated otherwise, these potential amplitudes will be random variables. Since we are solving for ϕ seeking an equation for the wave action N, we must relate N to ϕ. Accurate to second order in ε and η (see Andrews & McIntyre 1978 for a general expression for N), one has $N = E/\sigma$ for a monochromatic wave of surface elevation variance E and intrinsic frequency σ. Following the common usage in non-accelerated reference frames, the gravity g is left out, so that the action has units of metres squared times seconds. For general waves, E may be written as

$$E(t) = \langle(\zeta_0 + \zeta_1 + \zeta_2 + \cdots)^2\rangle = \langle \zeta_0^2 + 2\zeta_0\zeta_1 + (\zeta_1^2 + 2\zeta_0\zeta_2) + \cdots \rangle, \tag{2.8}$$

where $\langle\cdot\rangle$ denotes an average over flow realizations, and ζ_i is the surface elevation solution of order η^i. Terms of like order in η have been grouped. Each of these terms may be expanded in the form

$$\langle \zeta_i \zeta_j \rangle = \sum_{\boldsymbol{k}_i, \boldsymbol{k}_j, s_i, s_j} \left\langle Z^{s_i}_{i,\boldsymbol{k}_i} Z^{s_j}_{j,\boldsymbol{k}_j} \mathrm{e}^{\mathrm{i}[(\boldsymbol{k}_i+\boldsymbol{k}_j)\cdot\boldsymbol{x} - \Omega(\boldsymbol{k}_i,\boldsymbol{k}_j,s_i,s_j)t]} \right\rangle = 2\mathrm{Re}\left(\sum_{\boldsymbol{k}} \langle Z^{+}_{i,\boldsymbol{k}} Z^{-}_{j,-\boldsymbol{k}} \rangle \right). \tag{2.9}$$

For free wave components, the elevation amplitude is proportional to the velocity potential amplitude:

$$Z^{s}_{j,\boldsymbol{k}} = \mathrm{i}s\sigma \Phi^{s}_{j,\boldsymbol{k}}/g. \tag{2.10}$$

The contribution of the complex-conjugate pairs of components $(\boldsymbol{k}, +)$ and $(-\boldsymbol{k}, -)$ are combined so that the covariance $F^{\Phi}_{i,j}(\boldsymbol{k})$ corresponds to waves with wavenumber magnitude k propagating in the direction of $\boldsymbol{k}$. In the limit of small wavenumber separation, a continuous slowly varying cross-spectrum can be defined (e.g. Priestley 1981, ch. 11; see also AH),

$$F^{\Phi}_{i,j}(\boldsymbol{k}, t) = \lim_{|\Delta k|\to 0} \frac{2\mathrm{Re}\langle \Phi^{+}_{i,\boldsymbol{k}} \Phi^{-}_{j,-\boldsymbol{k}} \rangle}{\Delta k_x \Delta k_y}. \tag{2.11}$$

The definition of all spectral densities is chosen so that the integral over the entire wavenumber plane yields the covariance of ϕ_i and ϕ_j.

Finally, $N_{i,j}(\boldsymbol{k}, t)$ is defined as the $(i + j)$th-order depth-integrated wave action contribution from correlation between ith- and jth-order components with wavenumber k. From (2.8) and (2.10)

$$N_{i,j}(\boldsymbol{k}, t) = \frac{k}{\sigma} F^{\Phi}_{i,j}(\boldsymbol{k}, t) \tanh(kH). \tag{2.12}$$

Omitting the time dependence,

$$N(\boldsymbol{k}) = \sum_{i=0}^{\infty} N_i(\boldsymbol{k}) = \sum_{i=0}^{\infty} \sum_{j=0}^{i} N_{i,i-j}(\boldsymbol{k}). \tag{2.13}$$

Defining $G_{\boldsymbol{l}}$ as the amplitude of the Fourier component of wavenumber $\boldsymbol{l}$, the bottom elevation is given by

$$h(\boldsymbol{x}) = \sum_{\boldsymbol{l}} G_{\boldsymbol{l}} \mathrm{e}^{\mathrm{i}\boldsymbol{l}\cdot[\boldsymbol{x} + \boldsymbol{U}t]}, \tag{2.14}$$

with a summation on the entire wavenumber plane. Because h is real, $\overline{G_{-\boldsymbol{l}}} = G_{\boldsymbol{l}}$. The bottom elevation spectrum is given by

$$F^{B}(\boldsymbol{l}) = \lim_{|\Delta l|\to 0} \frac{\langle G_{\boldsymbol{l}} G_{-\boldsymbol{l}} \rangle}{\Delta l_x \Delta l_y}, \tag{2.15}$$

https://doi.org/10.1017/S0022112006004484 Published online by Cambridge University Press

and satisfies

$$\int_{-\infty}^{\infty}\int_{-\infty}^{\infty} F^B(\boldsymbol{l})\,\mathrm{d}l_x\,\mathrm{d}l_y = \lim_{L\to\infty}\frac{1}{L^2}\int_{-L/2}^{L/2}\int_{-L/2}^{L/2} h^2(x,y)\,\mathrm{d}x\,\mathrm{d}y. \tag{2.16}$$

Now that the scene is set, we solve for the velocity potential ϕ in the frame of reference moving with the mean current, and use (2.12) to estimate the action spectral density at each successive order. In the course of this calculation, ϕ will appear as the sum of many terms, some of which are secular (these are the 'resonant terms' in Hasselmann's terminology), i.e. with amplitudes growing in time. All other terms are bounded in time and thus do not contribute to the long-term evolution of the wave spectrum, i.e. on the scale of several wave periods, and will be neglected (see Hasselmann 1962).

2.2. *Zeroth-order solution*

In the moving frame of reference, the governing equations for ϕ_0 are identical to those in the fixed frame in the absence of current. The solution is thus

$$\phi_0 = \sum_{\boldsymbol{k},s}\frac{\cosh(k(z+H))}{\cosh(kH)}\Phi^s_{0,\boldsymbol{k}}\mathrm{e}^{\mathrm{i}[\boldsymbol{k}\cdot\boldsymbol{x}-s\sigma t]}, \tag{2.17}$$

where the intrinsic frequency σ is the positive root of the linear dispersion relation,

$$\sigma^2 = gk\tanh(kH). \tag{2.18}$$

2.3. *First-order solution*

Surface nonlinearity becomes relevant at first order due to a coupling between the zeroth-order solution and current-induced first-order terms. The expansion of the surface boundary condition to order ε^2 gives, at $z=0$,

$$\frac{\partial\phi}{\partial t^2}+g\frac{\partial\phi}{\partial z} = -\zeta\frac{\partial^3\phi}{\partial t^2\partial z}-g\zeta\frac{\partial^2\phi}{\partial z^2}-\frac{\partial\zeta}{\partial t}\frac{\partial^2\phi}{\partial z\partial t}+\nabla\phi\cdot\left(g\nabla\zeta-\frac{\partial\nabla\phi}{\partial t}\right)-\frac{\partial\phi}{\partial z}\frac{\partial^2\phi}{\partial t\partial z} + c_1'(t)+O(\varepsilon^3). \tag{2.19}$$

The equations at order η are

$$\nabla^2\phi_1+\frac{\partial^2\phi_1}{\partial z^2}=0 \quad \text{for} \quad -H\leqslant z\leqslant 0, \tag{2.20}$$

$$\frac{\partial\phi_1}{\partial z} = -h\frac{\partial^2\phi_0}{\partial z^2}+\nabla\phi_0\cdot\nabla h+\frac{\partial h}{\partial t} \qquad \text{at} \qquad z=-H, \tag{2.21}$$

and, at $z=0$, expansion of (2.19) to first order in η yields

$$\begin{aligned}\frac{\partial^2\phi_1}{\partial t^2}+g\frac{\partial\phi_1}{\partial z} = {}& \overbrace{g\left(\nabla\phi_0\cdot\nabla\zeta_1-\zeta_1\frac{\partial^2\phi_0}{\partial z^2}\right)}^{\mathrm{I}}+\overbrace{g\left(\nabla\phi_1\cdot\nabla\zeta_0-\zeta_0\frac{\partial^2\phi_1}{\partial z^2}\right)}^{\mathrm{II}}\\ & -\nabla\phi_1\cdot\overbrace{\frac{\partial\nabla\phi_0}{\partial t}}^{\mathrm{III}}-\nabla\phi_0\cdot\overbrace{\frac{\partial\nabla\phi_1}{\partial t}}^{\mathrm{IV}}-\overbrace{\left(\frac{\partial\phi_1}{\partial z}+\frac{\partial\zeta_1}{\partial t}\right)\frac{\partial^2\phi_0}{\partial t\partial z}}^{\mathrm{V}}-2\overbrace{\frac{\partial\phi_0}{\partial z}\frac{\partial^2\phi_1}{\partial t\partial z}}^{\mathrm{VI}}\\ & -\zeta_1\overbrace{\frac{\partial^3\phi_0}{\partial t^2\partial z}}^{\mathrm{VII}}-\zeta_0\overbrace{\frac{\partial^3\phi_1}{\partial t^2\partial z}}^{\mathrm{VIII}}+NL_1.\end{aligned} \tag{2.22}$$

https://doi.org/10.1017/S0022112006004484 Published online by Cambridge University Press

The term NL_1 corresponds to quadratic products of the zeroth-order solution and is given explicitly by Hasselmann (1962, equations 1.11–1.12) with the addition of the spatially uniform term $c_1'(t)$ (e.g. Longuet-Higgins 1950). NL_1 will be neglected thanks to the choice $\varepsilon < \eta$ as it gives no resonance below the third order in η.

However, the first-order system of equations is nonlinear due to the surface boundary condition (2.22). The right-hand-side terms have been kept because the current is distorted by the bottom and gives rise to a velocity potential ϕ_{1c} and surface displacement ζ_{1c} that are of the order of η times the Froude number $Fr = U/(gh)^{1/2}$, and may thus be larger than ϕ_0 and ζ_0, even though the mean convective velocity potential $\boldsymbol{U}\cdot\boldsymbol{x}$ has been removed by the change of frame of reference. Therefore the contribution of this motion to the terms I–VIII must be retained at order η. We thus first solve for (ϕ_{1c}, ζ_{1c}), which is the solution when $\partial h/\partial t$ only is retained in the right-hand sides. This mean current perturbation is given by Kirby (1988, equation 2.9) for a sinusoidal bottom. With a more general bottom, it is

$$\phi_{1c} = \mathrm{i}\sum_{l} \boldsymbol{U}\cdot\boldsymbol{l}\,\frac{G_l}{l\alpha_l}\{\beta_l \cosh[l(z+H)] + \alpha_l \sinh[l(z+H)]\}\mathrm{e}^{\mathrm{i}\boldsymbol{l}\cdot(\boldsymbol{x}+\boldsymbol{U}t)}, \tag{2.23}$$

where

$$\alpha_l = \frac{(\boldsymbol{U}\cdot\boldsymbol{l})^2}{gl} - \tanh(lh), \tag{2.24}$$

and

$$\beta_l = 1 - \tanh(lh)\frac{(\boldsymbol{U}\cdot\boldsymbol{l})^2}{gl}. \tag{2.25}$$

The corresponding surface elevation oscillations, given by (2.3), are second order in the Froude number $Fr = U/(gh)^{1/2}$, and 180° out of phase with the bottom oscillations for slow currents when $\alpha < 0$ (Kirby 1988, equation 2.10),

$$\zeta_{1c} = \sum_{l} \frac{(\boldsymbol{U}\cdot\boldsymbol{l})^2 G_l}{g\alpha_l \cosh(lh)}\mathrm{e}^{\mathrm{i}\boldsymbol{l}\cdot(\boldsymbol{x}+\boldsymbol{U}t)}. \tag{2.26}$$

From (2.23), the following expressions are derived, to be used in (2.22):

$$\phi_{1c}(z=0) = \mathrm{i}\sum_{l} \boldsymbol{U}\cdot\boldsymbol{l}\,\frac{G_l}{l\alpha_l \cosh(lh)}\mathrm{e}^{\mathrm{i}\boldsymbol{l}\cdot(\boldsymbol{x}+\boldsymbol{U}t)}, \tag{2.27}$$

$$\frac{\partial\phi_{1c}}{\partial z}(z=0) = \frac{\partial\zeta_{1c}}{\partial t} = \mathrm{i}\sum_{l} (\boldsymbol{U}\cdot\boldsymbol{l})^3\,\frac{G_l}{g\alpha_l \cosh(lh)}\mathrm{e}^{\mathrm{i}\boldsymbol{l}\cdot(\boldsymbol{x}+\boldsymbol{U}t)}. \tag{2.28}$$

We can now obtain the general solution to our equations (2.20)–(2.22) by the following superposition of the previous solution with free and bound (i.e. non-resonant) wave components, with amplitudes $\Phi^{s}_{1,\boldsymbol{k}}$ and $\Phi^{\mathrm{si},s}_{1,\boldsymbol{k}}$ respectively,

$$\phi_1 = \phi_{1c} + \sum_{\boldsymbol{k},s}\left[\frac{\cosh[k(z+H)]}{\cosh(kH)}\Phi^{s}_{1,\boldsymbol{k}}(t) + \frac{\sinh[k(z+H)]}{\cosh(kH)}\Phi^{\mathrm{si},s}_{1,\boldsymbol{k}}(t)\right]\mathrm{e}^{\mathrm{i}\boldsymbol{k}\cdot\boldsymbol{x}}, \tag{2.29}$$

where the last two terms correspond to the solution to (2.19)–(2.21) when the term $\partial h/\partial t$ is removed.

Substitution of (2.29) in the bottom boundary condition (2.21) yields

$$\frac{k}{\cosh(kH)}\Phi^{\mathrm{si},s}_{1,\boldsymbol{k}}(t) = -\sum_{\boldsymbol{k}'}\frac{\boldsymbol{k}'\cdot\boldsymbol{k}}{\cosh(k'H)}\Phi^{s}_{0,\boldsymbol{k}'}G_{\boldsymbol{k}-\boldsymbol{k}'}\mathrm{e}^{\mathrm{i}[(\boldsymbol{k}-\boldsymbol{k}')\cdot\boldsymbol{U}-s\sigma']t}. \tag{2.30}$$

https://doi.org/10.1017/S0022112006004484 Published online by Cambridge University Press

Substituting (2.29) in the surface boundary condition (2.22) yields an equation for $\Phi^s_{1,\boldsymbol{k}}$. Using $\omega = \sigma + \boldsymbol{k}\cdot\boldsymbol{U}$ and $\omega' = \sigma' + \boldsymbol{k}'\cdot\boldsymbol{U}$, it is written

$$\left(\frac{\mathrm{d}^2}{\mathrm{d}t^2} + \sigma^2\right)\Phi^s_{1,\boldsymbol{k}}(t) = \sum_{\boldsymbol{k}'} M^s(\boldsymbol{k},\boldsymbol{k}')\Phi_{0,\boldsymbol{k}'}G_{\boldsymbol{k}-\boldsymbol{k}'}\mathrm{e}^{\mathrm{i}[\boldsymbol{k}\cdot\boldsymbol{U}-s\omega']t}, \tag{2.31}$$

with

$$M^s(\boldsymbol{k},\boldsymbol{k}') = \{gk - [\boldsymbol{k}\cdot\boldsymbol{U} - s\omega']^2\tanh(kH)\}\frac{\boldsymbol{k}'\cdot\boldsymbol{k}}{k}\frac{\cosh(kH)}{\cosh(k'H)} + M^s_{c1}(\boldsymbol{k},\boldsymbol{k}'), \tag{2.32}$$

where M^s_{c1} is given by all the right-hand-side terms in (2.22) and thus corresponds to the scattering induced by current and current-induced surface elevation variations. Anticipating resonance, we only give the form of $M^s_{c1} = M^s_c$ for $\sigma = \sigma' - s\boldsymbol{l}\cdot\boldsymbol{U}$, with $\boldsymbol{l} = \boldsymbol{k} - \boldsymbol{k}'$,

$$M^s_c(\boldsymbol{k},\boldsymbol{k}') = \frac{\left\{sg^2\boldsymbol{U}\cdot\boldsymbol{l}(\sigma'\overset{(a)}{\boldsymbol{l}\cdot\boldsymbol{k}} + \sigma\overset{(b)}{\boldsymbol{l}\cdot\boldsymbol{k}'}) - (\boldsymbol{U}\cdot\boldsymbol{l})^2[g^2\overset{(c)}{\boldsymbol{k}\cdot\boldsymbol{k}'} - \overbrace{\sigma\sigma'(\sigma\sigma' + (\boldsymbol{U}\cdot\boldsymbol{l})^2)}^{(d)}]\right\}}{lg^2\alpha_l\cosh(lh)}, \tag{2.33}$$

in which the term (a) is given by the term II in (2.19), (b) is given by III and IV, (c) is given by I, and (d) is given by V–VIII. Because we are first solving the problem to order η, it is natural that our solution is a linear superposition of the solutions found by Kirby (1988) for a single bottom component. Indeed, $M_c(\boldsymbol{k},\boldsymbol{k}') = -4\omega\Omega_c/D$, with Ω_c the interaction coefficient of Kirby (1988, equation 4.22b) and D his bottom amplitude; here $G_l = \mathrm{i}D/2$.

The solution to the forced harmonic oscillator equation (2.31) is

$$\Phi^s_{1,\boldsymbol{k}}(t) = \sum_{\boldsymbol{k}'} M^s(\boldsymbol{k},\boldsymbol{k}')\Phi^s_{0,\boldsymbol{k}'}G_{\boldsymbol{k}-\boldsymbol{k}'}f_1(\sigma, \boldsymbol{l}\cdot\boldsymbol{U} - s\sigma'; t), \tag{2.34}$$

where $\boldsymbol{l} = \boldsymbol{k} - \boldsymbol{k}'$, and the function f_1 is defined in Appendix A.

2.3.1. *First-order action*

The lowest-order scattering contribution to the wave action equation involves the order-η covariances

$$F^{\Phi}_{1,0,\boldsymbol{k}} + F^{\Phi}_{0,1,\boldsymbol{k}} = 4\lim_{|\Delta k|\to 0}\frac{\mathrm{Re}\langle\Phi^+_{0,\boldsymbol{k}}\Phi^-_{1,-\boldsymbol{k}}\rangle}{\Delta k_x\Delta k_y}. \tag{2.35}$$

Including only the secular terms, we obtain

$$\langle\Phi^+_{0,\boldsymbol{k}}\Phi^-_{1,-\boldsymbol{k}}\rangle = \sum_{\boldsymbol{k}'} M^+(\boldsymbol{k},\boldsymbol{k}')\langle\Phi^+_{0,\boldsymbol{k}'}\Phi^-_{0,-\boldsymbol{k}}G_{\boldsymbol{k}-\boldsymbol{k}'}\rangle f_1(\sigma, \boldsymbol{l}\cdot\boldsymbol{U} - \sigma'; t)\mathrm{e}^{\mathrm{i}\sigma t}. \tag{2.36}$$

Although this term was assumed to be zero in AH, it is not zero for sinusoidal bottoms with partially standing waves, and may become significant at resonance due to the function f_1. In uniform conditions, the time evolution of the wave field requires that the non-stationarity must come into play. Thus $\gamma \approx \eta$ and the non-stationary term is given by AH (their Appendix D):

$$\frac{\partial\left[N^{\mathrm{ns}}_{1,0}(\boldsymbol{k}) + N^{\mathrm{ns}}_{0,1}(\boldsymbol{k})\right]}{\partial t} = -\frac{\partial N_0(\boldsymbol{k})}{\partial t}. \tag{2.37}$$

https://doi.org/10.1017/S0022112006004484 Published online by Cambridge University Press

In order to simplify the discussion, we shall briefly assume that there is no current and that the waves are unidirectional. In that case, $\boldsymbol{k}' = -\boldsymbol{k}$ and $M(\boldsymbol{k}, \boldsymbol{k}') = -gk^2/\cosh^2(kH)$. Substituting (2.36) in (2.12) and combining it with (2.37) yields the action balance

$$\frac{\partial N_{0,\boldsymbol{k}}}{\partial t} = \frac{\partial}{\partial t}\left[\frac{k}{g\sigma}\tanh(kH)\left(F^{\Phi}_{1,0,\boldsymbol{k}} + F^{\Phi}_{0,1,\boldsymbol{k}}\right)\right] = \mathrm{Im}\left(\frac{-4k^2\sigma}{2g\cosh^2(kH)}\langle \Phi^{+}_{0,\boldsymbol{k}}\Phi^{-}_{0,\boldsymbol{k}}G_{-2k}\rangle\right), \tag{2.38}$$

with Im denoting the imaginary part.

Using $N(\boldsymbol{k}) = N_0(\boldsymbol{k})[1+O(\eta)]$ and taking the limit to continuous surface and bottom spectra yields

$$\frac{\partial N(\boldsymbol{k})}{\partial t} = S_1(\boldsymbol{k}) = \int_0^{2\pi} \frac{4\boldsymbol{k}\cdot\boldsymbol{k}'}{2g\cosh(kH)\cosh(k'H)}\mathrm{Im}[Z(\boldsymbol{k}, \boldsymbol{k}')]\,\mathrm{d}k'_x\,\mathrm{d}\theta', \tag{2.39}$$

with the mixed surface bottom bispectrum Z defined by

$$Z(\boldsymbol{k}, \boldsymbol{k}') = \lim_{\Delta\boldsymbol{k}\to\infty}\left\langle \frac{\Phi^{+}_{1,\boldsymbol{k}}\Phi^{-}_{1,-\boldsymbol{k}'}G_{-k-k'}}{\Delta\boldsymbol{k}\Delta\theta'}\right\rangle, \tag{2.40}$$

with $\boldsymbol{k} = k(\cos\theta, \sin\theta)$ and $\boldsymbol{k}' = k(\cos\theta', \sin\theta')$. Z is similar to a classical bispectrum (e.g. Herbers *et al.* 2003) with one surface wave amplitude replaced by a bottom amplitude, and a similar expression is found for a non-zero current. The action balance (2.39) is generally not closed, as Z is a function of the relative wave phases, which are not available in a phase-averaged model. The same type of coupling, though due to the large-scale topography, also occurs in the stochastic equations for nonlinear wave evolution derived by Janssen, Herbers & Battjes (2006).

The contribution of the mixed bispectrum will thus be evaluated below, in order to investigate in which cases it may be neglected or parameterized. If it is non-zero, the slow evolution time scale T/γ is of order T/η, with T a typical wave period and $\gamma = T\max\{S_1/N\}$. It is expected that the correlations represented by this bispectrum are negligible for waves with amplitudes that vary slowly in space over a random bottom, provided that the evolution space scale C_gT/γ is larger than the bottom correlation length. Such waves scattered over one region have no phase correlation with the bottom once they have propagated beyond the bottom correlation length, and any slow spectral evolution on these scales must be due to higher-order interactions, with a time scale of at least T/η^2. For two-dimensional (cylindrical) bottoms and without current, Magne *et al.* (2005*a*) have proved that the time scale for the mean evolution of an incident wavetrain over any bottom is indeed T/η^2, in the absence of other waves propagating from the area of interest, with a source term compatible with the second-order theory given below.

2.3.2. *Second-order action*

From the expansion (2.13), the second-order action is $N_2(\boldsymbol{k}) = N_{1,1}(\boldsymbol{k}) + N_{0,2}(\boldsymbol{k}) + N_{2,0}(\boldsymbol{k})$. All these terms are of the same order in η and must all be evaluated. In particular, neglecting the last two terms, which contribute the linear term $-N(\boldsymbol{k})$ in (2.51), would lead to a non-conserving form of the action equation, similar to the first-order amplitude evolution equations of Miles (1981) or Pihl *et al.* (2002). For the same reason Hasselmann (1962) had to carry his derivation to order ε^5 in order to obtain the equation that now bears his name, because his first resonant term $N_{3,3}$ is of the same order as $N_{5,1}$.

https://doi.org/10.1017/S0022112006004484 Published online by Cambridge University Press

Here $N_{1,1}$ can be estimated from ϕ_1, using the covariance of the velocity potential amplitudes (2.11),

$$F^{\Phi}_{1,1}(\boldsymbol{k}) = 2 \lim_{|\Delta k|\to 0} \frac{\mathrm{Re}\langle \Phi^{+}_{1,\boldsymbol{k}} \Phi^{-}_{1,-\boldsymbol{k}} \rangle}{\Delta k_x \Delta k_y}. \tag{2.41}$$

Using (2.34), (2.41) can be re-written as

$$\frac{\Phi^{+}_{1,\boldsymbol{k}} \Phi^{-}_{1,-\boldsymbol{k}}}{\Delta \boldsymbol{k}} = \sum_{\boldsymbol{k}'} |M^{+}(\boldsymbol{k},\boldsymbol{k}')|^2 \frac{\langle |\Phi^{+}_{0,\boldsymbol{k}'}|^2 \rangle}{\Delta \boldsymbol{k}'} \frac{\langle |G_{\boldsymbol{k}-\boldsymbol{k}'} G_{-\boldsymbol{k}+\boldsymbol{k}'}|^2 \rangle}{\Delta \boldsymbol{k}} |f_1(\sigma, \boldsymbol{l}\cdot\boldsymbol{U} - \sigma'; t)|^2 \Delta \boldsymbol{k}'. \tag{2.42}$$

Taking the limit of (2.42) when $\Delta \boldsymbol{k} \to 0$ gives

$$F^{\Phi}_{1,1}(t,\boldsymbol{k}) = \int_{-\infty}^{\infty}\int_{-\infty}^{\infty} |M^{+}(\boldsymbol{k},\boldsymbol{k}')|^2 F^{\Phi}_{1,1}(\boldsymbol{k}') F^{B}(\boldsymbol{k}-\boldsymbol{k}') |f_1(\sigma, \boldsymbol{l}\cdot\boldsymbol{U} - \sigma'; t)|^2 \,\mathrm{d}k'_x \,\mathrm{d}k'_y. \tag{2.43}$$

Owing to the singularity in f_1, and assuming that the rest of the integrand can be approximated by an anlytical function in the neighbourhood of the singularity $\omega' = \omega$, which requires both bottom and surface elevation spectra to be continuous, the integral can be evaluated by using

$$\langle f_1(\sigma, \boldsymbol{l}\cdot\boldsymbol{U} - \sigma'; t) f_1(\sigma, -\boldsymbol{l}\cdot\boldsymbol{U} + \sigma'; t)\rangle = \frac{\pi t}{4\sigma^2}[\delta(\sigma' - (\sigma + \boldsymbol{l}\cdot\boldsymbol{U})) + O(1)]; \tag{2.44}$$

δ is the one-dimensional Dirac distribution, infinite where the argument is zero, and such that $\int \delta(x) A(x)\,\mathrm{d}x = A(0)$ for any continuous function A. In order to remove that singularity, the argument of δ maye be re-written as $\omega' - \omega$, making explicit all the dependences on k'. Evaluation of the δ function is then performed by changing integration variables (k'_x, k'_y) to (ω', θ'), with a Jacobian $k'\partial k'/\partial\omega' = k'^2/(k' C'_g + \boldsymbol{k}'\cdot\boldsymbol{U})$. We thus have

$$F^{\Phi}_{1,1}(t,\boldsymbol{k}) = \frac{\pi t}{2\sigma^2} \int_0^{2\pi}\int_{\omega'} |M^{+}(\boldsymbol{k},\boldsymbol{k}')|^2 F^{\Phi}_{1,1}(\boldsymbol{k}') \frac{k' F^{B}(\boldsymbol{k}-\boldsymbol{k}')}{C'_g + \boldsymbol{k}'\cdot\boldsymbol{U}} \delta(\omega' - \omega)\,\mathrm{d}\omega'\,\mathrm{d}\theta' + O(1). \tag{2.45}$$

When $\omega = \omega'$, the integrand simplifies: $M^{s}(\boldsymbol{k},\boldsymbol{k}')$ is equal to $M(\boldsymbol{k},\boldsymbol{k}')$, defined by

$$M(\boldsymbol{k},\boldsymbol{k}') = \frac{g\boldsymbol{k}\cdot\boldsymbol{k}'}{\cosh(kH)\cosh(k'H)} + M_c(\boldsymbol{k},\boldsymbol{k}') \equiv M_b(\boldsymbol{k},\boldsymbol{k}') + M_c(\boldsymbol{k},\boldsymbol{k}'), \tag{2.46}$$

with $M_c = M^{+}_{c}$ given by (2.33). Using the relation (2.12) between velocity potential and action, and evaluating the integral over ω', one obtains

$$N_{1,1}(t,\boldsymbol{k}) = \frac{\pi t}{2} \int_0^{2\pi} M^2(\boldsymbol{k},\boldsymbol{k}') \frac{N_0(\boldsymbol{k}')}{\sigma\sigma'} F^{B}(\boldsymbol{k}-\boldsymbol{k}') \frac{k'^2}{k' C'_g + \boldsymbol{k}'\cdot\boldsymbol{U}}\,\mathrm{d}\theta' + O(1). \tag{2.47}$$

Again we note the correspondance with the theory of Kirby (1988, equation 4.21). Specifically, $M(\boldsymbol{k},\boldsymbol{k}') = -4\omega\Omega_c/D$, with Ω_c being Kirby's interaction coefficient.

After calculations detailed in Appendix B, ϕ_2 yields the following contribution to the wave action:

$$N_{2,0}(\boldsymbol{k}) + N_{0,2}(\boldsymbol{k}) = -\frac{\pi t}{2} \int_0^{2\pi} M^2(\boldsymbol{k},\boldsymbol{k}') F^{B}(\boldsymbol{k}-\boldsymbol{k}') \frac{N_0(\boldsymbol{k})}{\sigma\sigma'} \frac{k'^2}{k' C'_g + \boldsymbol{k}'\cdot\boldsymbol{U}}\,\mathrm{d}\theta' + O(1), \tag{2.48}$$

in which $\sigma' = \sigma - \boldsymbol{l}\cdot\boldsymbol{U}$, $\sigma'^2 = gk'\tanh(kH)$, and $C'_g = \sigma'(1/2 + k'H/\sinh(2k'H))/k'$.

https://doi.org/10.1017/S0022112006004484 Published online by Cambridge University Press

2.4. *Action and momentum balances*

We shall neglect the first-order action contribution N_1 given by (2.39). The solvability condition imposed on the action spectrum is that N_2 remains an order η^2 smaller than N_0 for all times. Thus all secular terms of order η^2 must cancel. Combining (2.37), (2.47), and (2.48) gives

$$-\frac{\mathrm{d}N_0(\boldsymbol{k})}{\mathrm{d}t}+\frac{\pi}{2}\int_0^{2\pi} M^2(\boldsymbol{k},\boldsymbol{k}')F^B(\boldsymbol{k}-\boldsymbol{k}')\frac{N_0(\boldsymbol{k}')-N_0(\boldsymbol{k})}{\sigma\sigma'}\frac{k'^2}{k'C_g'+\boldsymbol{k}'\cdot\boldsymbol{U}}\,\mathrm{d}\theta'. \tag{2.49}$$

Since N_2 remains small, $N(\boldsymbol{k})=N_0(\boldsymbol{k})[1+O(\eta^2)]$, and

$$\frac{\mathrm{d}N(\boldsymbol{k})}{\mathrm{d}t}=S_{\mathrm{bscat}}(\boldsymbol{k}), \tag{2.50}$$

with the spectral action source term,

$$S_{\mathrm{bscat}}(\boldsymbol{k})=\frac{\pi}{2}\int_0^{2\pi}\frac{k'^2M^2(\boldsymbol{k},\boldsymbol{k}')}{\sigma\sigma'(k'C_g'+\boldsymbol{k}'\cdot\boldsymbol{U})}F^B(\boldsymbol{k}-\boldsymbol{k}')[N(\boldsymbol{k}')-N(\boldsymbol{k})]\,\mathrm{d}\theta', \tag{2.51}$$

where $\sigma'=\sigma+\boldsymbol{l}\cdot\boldsymbol{U}$ and $\boldsymbol{k}=\boldsymbol{k}'+\boldsymbol{l}$. This interaction rule was given by Kirby (1988). The only waves that can interact share the same absolute frequency $\omega=\sigma+\boldsymbol{k}\cdot\boldsymbol{U}=\sigma'+\boldsymbol{k}'\cdot\boldsymbol{U}$. For a given $\boldsymbol{k}$ and without current, the resonant $\boldsymbol{k}'$ and $\boldsymbol{l}$ lie on circles in the wavenumber plane (see AH). The current slightly modifies this geometric property. For $U\ll C_g$ the circles become ellipses (Appendix C).

For a given value of ω, one may obtain the source term integrated over all directions,

$$\begin{aligned}S_{\mathrm{bscat}}(\omega)&=\int_0^{2\pi}kS_{\mathrm{bscat}}(\boldsymbol{k})\frac{\partial k}{\partial\omega}\mathrm{d}\theta=\int_0^{2\pi}S_{\mathrm{bscat}}(\omega,\theta)\,\mathrm{d}\theta\\&=\int_0^{2\pi}\int_0^{2\pi}\frac{\pi}{2}\frac{k^2k'^2M^2(\boldsymbol{k},\boldsymbol{k}')F^B(\boldsymbol{k}-\boldsymbol{k}')}{\sigma\sigma'(k'C_g'+\boldsymbol{k}'\cdot\boldsymbol{U})(kC_g+\boldsymbol{k}\cdot\boldsymbol{U})}[N(\boldsymbol{k}')-N(\boldsymbol{k})]\,\mathrm{d}\theta'\,\mathrm{d}\theta\\&=\int_0^{2\pi}\int_0^{2\pi}\frac{\pi}{2}\frac{M^2(\boldsymbol{k},\boldsymbol{k}')F^B(\boldsymbol{k}-\boldsymbol{k}')}{\sigma\sigma'}\left[\frac{k^2N(\omega,\theta')}{kC_g+\boldsymbol{k}\cdot\boldsymbol{U}}-\frac{k'^2N(\omega,\theta)}{k'C_g'+\boldsymbol{k}'\cdot\boldsymbol{U}}\right]\mathrm{d}\theta'\,\mathrm{d}\theta.\end{aligned} \tag{2.52}$$

This expression is antisymmetric, multiplied by -1 when θ and θ' are exchanged. For continuous integrands the order of the integrals may be switched and thus for any bottom and wave spectra $S_{\mathrm{bscat}}(\omega)=0$. In other words, the 'source term' is instead an 'exchange term', and conserves the wave action at each absolute frequency. This conservation is consistent with the general wave action conservation theorem proved by Andrews & McIntyre (1978), which states that there is no flux of action through an unperturbed boundary (here the bottom). It also appears that ω and θ are natural spectral coordinates in which the scattering source term takes a symmetric form. Finally, we may consider the equilibrium spectra that satisfy $S_{\mathrm{bscat}}(\boldsymbol{k})=0$ for all $\boldsymbol{k}$. Without a current, an equilibrium exists when either $N(\omega,\theta)$ or $N(\boldsymbol{k})$ is isotropic. With a current, the scattering term is uniformly zero if and only if the spectral densities in $\boldsymbol{k}$-space, $N(\boldsymbol{k})$, are uniform along the curves of constant ω.

The source term S_{bscat} may also be re-written in a form corresponding to that in AH, which now appears much less elegant:

$$S_{\mathrm{bscat}}(\boldsymbol{k})=\int_0^{2\pi}K(k,k',H)F^B(\boldsymbol{k}-\boldsymbol{k}')[N(\boldsymbol{k}')-N(\boldsymbol{k})]\,\mathrm{d}\theta', \tag{2.53}$$

https://doi.org/10.1017/S0022112006004484 Published online by Cambridge University Press

with

$$K(k,k',H)=\frac{\pi k'^2M^2(k,k')}{2\sigma\sigma'(k'C'_g+\boldsymbol{k}'\cdot\boldsymbol{U})}=\frac{4\pi\sigma kk'^3\cos^2(\theta-\theta')[1+O(Fr)]}{\sinh(2kH)[2k'H+\sinh(2k'H)(1+2\boldsymbol{k}'\cdot\boldsymbol{U}/\sigma')]}. \tag{2.54}$$

One may wonder how large the current-induced scattering represented by M_c is, our (2.33), compared to the bottom-induced scattering represented by M_b. Since $\sigma'=\sigma+(\boldsymbol{U}\cdot\boldsymbol{l})$, the (a) and (b) terms in the numerator of (2.33) for M_c almost cancel for small Froude numbers, and the $(a)+(b)$ part is of order Fr^2. Thus M_c is generally an order Fr^2 smaller than M_b. For $\boldsymbol{k}$ and $\boldsymbol{k}'$ in opposite directions (i.e. back-scattering), the $(a)+(b)$ part is generally smaller, going to zero in the long-wave limit $lH\ll1$. Thus, for back-scattering and $lH\ll1$ the numerator in M_c is dominated by (c). Interestingly (c) formally comes from the modulations of the surface elevation ζ_{1c} so that the $O(Fr^2)$ elevation modulation may be as important as the $O(Fr)$ current modulation for this back-scattering situation. The relative magnitudes of M_b and M_c thus depend on $Fr(l)=(\boldsymbol{U}\cdot\boldsymbol{l})/[gl\tanh(lH)]^{1/2}$ that appears in $(\boldsymbol{U}\cdot\boldsymbol{l})^2/(gl\alpha_l)=Fr^2(l)/[Fr^2(l)-1]$. This l-scale Froude number may be larger than 1, in which case the scattered waves are swept downstream by the current, and M_c may be larger than M_b. In the long-wave limit, $Fr(l)=Fr$ and for $(1-Fr)\ll1$, $M_c>M_b$. For oblique scattering, the $(a)+(b)$ term may dominate the numerator of M_c and the situation is more complex. Nevertheless, for Froude numbers typical of continental shelf situations, say $0<Fr<0.4$, M_c may usually be neglected since its $O(Fr^2)$ correction to M_b corresponds to only a few percent of the reflection. Obvious exceptions are cases in which M_b is zero, such as when $\boldsymbol{k}$ and $\boldsymbol{k}'$ are perpendicular.

Finally, we may also write the evolution equation for the wave pseudo-momentum $\boldsymbol{M}^w=\rho_w g\int\boldsymbol{k}N(\boldsymbol{k})\mathrm{d}\boldsymbol{k}$ (see Andrews & McIntyre 1978), where ρ_w is the density of seawater. Introducing now the slow medium and wave field variations given by Kirby (1988), that do not interfere with the scattering process, except by probably reducing the surface-bottom bispectrum Z, one obtains an extension of the equation of Phillips (1977):

$$\frac{\partial M^w_\alpha}{\partial t}+\frac{\partial}{\partial x_\beta}\left[(U_\beta+C_{g\beta})M^w_\alpha\right]=-\tau^{\mathrm{bscat}}_\alpha-M^w_\beta\frac{\partial U_\beta}{\partial x_\alpha}-\frac{M^w_\alpha}{k_\alpha}\frac{k\sigma}{\sinh 2kD}\frac{\partial D}{\partial x_\alpha}, \tag{2.55}$$

with the dummy indices α and β denoting horizontal components x or y, and the scattering stress vector,

$$\tau^{\mathrm{bscat}}=-\rho_w g\int\boldsymbol{k}S_{\mathrm{bscat}}\,\mathrm{d}\boldsymbol{k}. \tag{2.56}$$

This stress has dimensions of force per unit area, and corresponds to the divergence of the wave pseudo-momentum flux. Based on the results of Longuet-Higgins (1967) and Hara & Mei (1987), this force does not contribute to the mean flow equilibrium, with the radiation stress divergence balanced by long waves (or wave set-up in stationary conditions), contrary to the initial proposition of Mei (1985). This force is thus a net flux of momentum through the bottom, arising from a correlation between the non-hydrostatic bottom pressure and the bottom slope. Although the part M_c of the coupling coefficient M given by (2.46) is formally due to scattering by the current modulations $\nabla\phi_{1c}$, and associated surface fluctuations ζ_{1c}, it should be noted that these motions and related pressures are correlated with the bottom slope in the same way as the part represented by M_b. Thus both terms contribute to this force τ^{bscat} which acts on the bottom and not on the mean flow.

https://doi.org/10.1017/S0022112006004484 Published online by Cambridge University Press

3. Wave scattering in two dimensions

Before considering the full complexity of the three-dimensional wave–bottom scattering in the presence of a current, we first examine the behaviour of the source term in the case of two-dimensional sinusoidal seabeds. Although the bottom spectrum is not continuous along the y-axis, continuity in x is sufficient for the use of (2.44) and the source term can be applied to remove these singularities, after proper transformation.

3.1. *Wave evolution equation in two dimensions*

We consider here a steady wave field in two dimensions with incident and reflected waves propagating along the x-axis. We shall consider in particular the case of m sinusoidal bars of amplitude b and height $2b$, with a wavelength $2\pi/l_0$. The bottom elevation is thus

$$\left.\begin{array}{l} h(x) = b\sin(l_0 x) \quad \text{for} \quad 0 < x < L, \\ h(x) = 0 \quad \text{otherwise.} \end{array}\right\} \tag{3.1}$$

Such a bottom is shown in figure 1 in § 2.1 for $m = 4$. This form is identical to that of the bottom profile chosen by Kirby (1988) but differs, for $0 < x < L$, by a $\pi/2$ phase shift from the bottom profile chosen by Mei (1985). The bottom spectrum is of the form

$$F^B(l_x, l_y) = F^{B2D}(l_x)\delta(l_y). \tag{3.2}$$

Owing to our normalization convention (2.16), the integral of the bottom spectrum is the bottom variance in the area where the source term is applied, here the region $0 < x < L$: the particular bottom given by (3.1) yields

$$F^{B2D}(l_x) = \frac{2\pi}{L}\left(\frac{1}{2\pi}\int_{-\infty}^{\infty} h(x)\mathrm{e}^{-\mathrm{i}l_x x}\,\mathrm{d}x\right)^2 = \frac{2b^2 l_0^2}{\pi L}\frac{\sin^2(l_x L/2)}{\left(l_0^2 - l^2\right)^2}, \tag{3.3}$$

with

$$F^{B2D}(\pm l_0) = \frac{mb^2}{4l_0} = \frac{b^2 L}{8\pi}. \tag{3.4}$$

Note that this is a double-sided spectrum, with only half of the bottom variance contained in the range $l_x > 0$. For a generic bottom, for which $h(x)$ does not go to zero at infinity, the spectrum is obtained using standard spectral analysis methods, for example, from the Fourier transform of the bottom auto-covariance function (see MAHR).

First, substituting (3.2) in (2.51) removes the angular integral in the source term. Taking $\boldsymbol{k} = (k_x, k_y)$, we have $l_y = k_y - k'_y = k\sin\theta - k'\sin\theta'$, thus $\mathrm{d}l_y = -k'_y\cos\theta'\mathrm{d}\theta'$, and

$$S_{\mathrm{bscat}}(\boldsymbol{k}, x) = \frac{\pi k' M^2(k, k') F^{B2D}(\boldsymbol{k} - \boldsymbol{k}')}{2\sigma\sigma'|\cos\theta'|(k'C'_g + \boldsymbol{k}'\cdot\boldsymbol{U})}[N(\boldsymbol{k}') - N(\boldsymbol{k})]. \tag{3.5}$$

Second, assuming now that waves propagate only along the x-axis, the wave spectral densities are of the form

$$N(k_x, k_y) = N(k_x, k_y)\delta(k_y) = N^{2D}(k)\delta(\theta - \theta_0)/k, \tag{3.6}$$

with $\theta_0 = 0$ for $k_x > 0$ and $\theta_0 = \pi$ for $k_x < 0$. Integrating over θ removes the singularities on k_y, and assuming a steady state one obtains

$$\left[\frac{k_x}{k}C_g + U_x\right]\frac{\partial N^{2D}}{\partial x}(k_x, x) = S^{2D}_{\mathrm{bscat}}(k_x, x), \tag{3.7}$$

https://doi.org/10.1017/S0022112006004484 Published online by Cambridge University Press

with

$$S^{2D}_{\mathrm{bscat}}(k_x, x) = \frac{\pi k' M^2(k, k') F^{B2D}(k_x - k'_x)}{2\sigma\sigma'(k'_x C'_g + k'_x U_x)} [N^{2D}(k'_x, x) - N^{2D}(k_x, x)]. \tag{3.8}$$

Although the present theory is formulated for random waves, there is no possible coupling between waves of different frequencies. Mathematically, it is possible to take the limit to an infinitely narrow wave spectrum, such that, $N^{2D}(k, x) = N(x)\delta(\omega - \omega_0) + N'(x)\delta(\omega' - \omega'_0)$ with $k_{0x} > 0$ and $k'_{0x} < 0$. Using $\partial\omega/\partial k = C_g + k_x U_x/|k_x|$, the resulting evolution equation is, omitting the 0 subscripts on k and k',

$$\left[\frac{k_x}{k} C_g + U_x\right] \frac{\partial N}{\partial x} = \frac{\pi M^2(k, k') F^{B2D}(k_x - k'_x)}{2\sigma\sigma'} \left[\frac{kN'}{kC_g + k_x U_x} - \frac{k'N}{k'C'_g + k'_x U_x}\right], \tag{3.9}$$

with a similar equation for N' obtained by exchanging C_g and C'_g, and k' and k, from which it is easy to verify that the total action is conserved.

The stationary evolution equation (3.7) only couples two wave components $N(k)$ and $N(k')$. For a uniform mean depth H, and uniform bottom spectrum F^B, as considered here, we thus have a linear system of two differential equations, that may be written in matrix form for any $k > 0$:

$$\frac{\mathrm{d}}{\mathrm{d}x} \begin{pmatrix} N(k) \\ N(k') \end{pmatrix} = q\mathbf{Q} \begin{pmatrix} N(k) \\ N(k') \end{pmatrix}, \tag{3.10}$$

with

$$q = \frac{\pi M^2(k, k') F^{B2D}(l)}{2\sigma\sigma' C g C g'}. \tag{3.11}$$

Defining $l = k_x - k'_x$, and the action advection velocities $V' = C'_g + k'_x U_x$ and $V = C_g + k_x U_x$, the terms of the non-dimensional matrix $\mathbf{Q}$ are given by

$$\left.\begin{aligned} (\mathbf{Q})_{1,1} &= -\frac{C_g C'_g}{V^2} \quad \text{and} \quad (\mathbf{Q})_{1,2} = \frac{C_g C'_g}{V V'}, \\ (\mathbf{Q})_{2,1} &= -\frac{C_g C'_g}{V'^2} \quad \text{and} \quad (\mathbf{Q})_{2,2} = \frac{C_g C'_g}{V V'}, \end{aligned}\right\} \tag{3.12}$$

where $(\mathbf{Q})_{i,j}$ is the ith row and jth column term of $\mathbf{Q}$. The general solution is thus

$$\begin{pmatrix} N(k, x) \\ N(k', x) \end{pmatrix} = \mathrm{e}^{q\mathbf{Q}x} \begin{pmatrix} N(k, 0) \\ N(k', 0) \end{pmatrix}. \tag{3.13}$$

The matrix exponential is classically the infinite series $\sum_{n=0}^{\infty} (q\mathbf{Q})^n / n!$, in which matrix multiplications are used. The reflection coefficient for the wave action is found using the boundary condition expressing the absence of incoming waves from beyond the bars, $N(k', L) = 0$, giving,

$$R_N = \frac{N(k', 0)}{N(k, 0)} = -(\mathrm{e}^{q\mathbf{Q}L})_{2,1} / (\mathrm{e}^{q\mathbf{Q}L})_{2,2}. \tag{3.14}$$

A reflection coefficient for the modulus of the wave amplitude predicted by the source term is thus

$$R_S = \left[\frac{\sigma' N(-k', 0)}{\sigma N(k, 0)}\right]^{1/2} = -\{\sigma'(\mathrm{e}^{q\mathbf{Q}L})_{2,1} / [\sigma(\mathrm{e}^{q\mathbf{Q}L})_{2,2}]\}^{1/2}. \tag{3.15}$$

The spatial variation of the amplitudes may be linear, oscillatory, or exponential, depending on whether the determinant of $\mathbf{Q}$ is zero, negative or positive, respectively.

https://doi.org/10.1017/S0022112006004484 Published online by Cambridge University Press

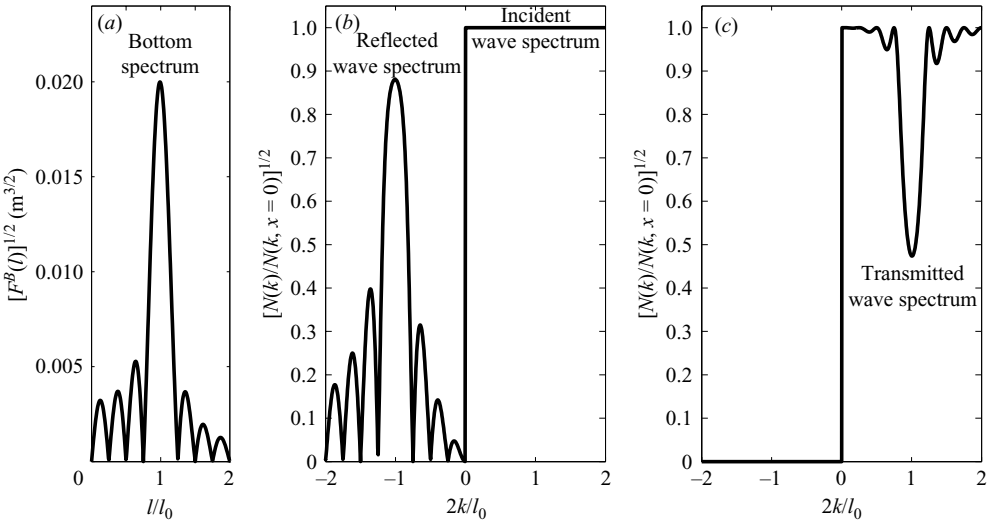


FIGURE 2. Bottom spectrum and evolution of a surface wave spectrum along a field of sinusoidal bars for $U=0$, $b=0.05\,\mathrm{m}$, $H=0.156\,\mathrm{m}$, so that $\eta=b/H=0.32$, and $l_0=2\pi$, $m=4$, so that $L=4\,\mathrm{m}$ (bottom shown in figure 1). (*a*) Square root of the bottom spectrum, (*b*) and (*c*) normalized square-root wave spectrum upwave (at $x<0$) and downwave (at $x>L$) of the bars, respectively. The incident spectrum ($k>0$ at $x=0$) is specified to be white (unform in wavenumbers).

That determinant is $C_g^2 C_g'^2 (V'-V)(V'^2+3VV'+4V^4)/V^4V'^3$, which is always of the sign of $V'-V$.

3.2. *Analytical solution for* $U=0$

In the absence of a mean current, $k'=-k$, and

$$(\boldsymbol{Q})_{1,1}=(\boldsymbol{Q})_{1,2}=-(\boldsymbol{Q})_{2,1}=-(\boldsymbol{Q})_{2,2}=1. \tag{3.16}$$

Thus $\boldsymbol{Q}^2=0$ so that its exponential is only the sum of two terms, $\mathrm{e}^{q\boldsymbol{Q}x}=(\boldsymbol{I}+q\boldsymbol{Q})x$, where $\boldsymbol{I}$ is the identity matrix. The solution to (3.9) is simply

$$N(k,x)=N(k,0)\left[\frac{-q(x-L)+1}{1+qL}\right], \tag{3.17}$$

$$N(-k,x)=N(k,0)\left[\frac{-q(x-L)}{1+qL}\right]. \tag{3.18}$$

An example of the spatial variation of the wave spectrum from $x=0$ to $x=L$ is shown in figure 2, for $U=0$, and a uniform (white) incident spectrum. The reflected wave energy (at $k<0$ in figure 2*a*) compensates the loss of energy in the transmitted spectrum (at $k>0$ in figure 2*b*).

For $k=l/2$, in the limit of small bar amplitudes, substituting (3.4) in (3.15) yields

$$R_S=(qL)^{1/2}+O(qL)=\frac{k^2bL}{2kH+\sinh(2kH)}+O(qL) \tag{3.19}$$

which is identical to Mei's (1985) equations (3.21)–(3.22) for exact resonance, in the limit of $qL\ll 1$, and also converges to the result of Davies & Heathershaw (1984) for that limit, which is a particular case of the more general result by Kreisel (1949). For fixed bar amplitudes, the reflection is significant if the bars occupy a length L

https://doi.org/10.1017/S0022112006004484 Published online by Cambridge University Press

longer than the localization length $1/q$. However, the reflection coefficient for the wave amplitude only increases with L as $[qL/(1+qL)]^{1/2}$, which is slower than the exponential asymptote given by Mei (1985) for sinusoidal bars, and predicted by Belzons, Guazzelli & Parodi (1988) from the lowest-order theory applied to a random bottom. The present inclusion of the correlations of second-order and zeroth-order terms may be thought of as the representation of multiple reflections that tend to increase the penetration length in the random medium.

3.3. *Effects of wave and bottom relative phases*

In the absence of currents, the energy exchange coefficient given by the source term always gives energy to the least energetic components, and thus the energy evolution is monotonic. The action source term (2.38) of order η, that was neglected so far, may have any sign, and may lead to oscillatory evolutions for the wave amplitudes, as predicted by Mei (1985) and observed by Hara & Mei (1987). Using Mei's (1985) notation, the amplitudes of the incident waves, reflected waves, and bottom undulations are $A = 2\sigma\Phi^{+}_{0,\boldsymbol{k}}/g$, $B = 2\sigma\Phi^{-}_{0,\boldsymbol{k}}/g$, and $D = -2\mathrm{i}G_{-2k}$, and the 'cutoff' frequency is

$$\Omega_0 = \frac{\sigma k D}{2\sinh(2kH)}. \tag{3.20}$$

At resonance, and for $U = 0$, it can be seen that the first-order energy product $\Phi^{+}_{0,\boldsymbol{k}}\Phi^{-}_{0,\boldsymbol{k}}G_{-2k}$ in (2.38) is equal to $\mathrm{i}AB^{\star}D/8$, in the limit of a large number of bars. Based on Mei's (1985) approximate solution, in the absence of waves coming from across the bars, this quantity is purely real so that its imaginary part is zero and the corresponding reflection coefficient R_{S1} is zero. For $U \neq 0$ this property remains, as can be seen by replacing Mei's (1985) solution with Kirby's (1988). However, similar correlation terms and bound terms were neglected in the second-order energy (Appendix B). These neglected terms, which do not modify the long-term evolution of the wave energy, are likely to be related to the oscillations of the amplitude across the bar field, observed by Hara & Mei (1987). Further, the bottom–surface bispectrum in S_1 may become significant if there is a large amount of wave energy coming from beyond the bars. This kind of situation, e.g. due to reflection over a beach, was discussed by Yu & Mei (2000).

In the absence of such a reflection, and away from resonance but for small values of the scattering strength parameter $\tau = (qL)^{1/2} = \Omega_0 L/C_g$, the imaginary part of $\Phi^{+}_{0,\boldsymbol{k}}\Phi^{-}_{0,\boldsymbol{k}}G_{-2k}$ is an order $(qL)^{1/2}$ smaller than the real part and thus contributes a negligible amount to the reflection.

3.4. *Source term and deterministic results for sinusoidal bars*

A deeper understanding of the Bragg scattering approximation is provided by the comparison of numerical estimations of R. A benchmark estimation for linear waves is provided by the step-wise model of Rey (1995) using integral matching conditions for the free propagating waves and evanescent modes at the step boundaries. This model is known to converge to the reflection coefficients given by an exact solution of Laplace's equation and the boundary conditions, in the limit of an infinite number of steps and evanescent modes. Calculations are performed here with 20 steps per bottom wavelength and three evanescent modes. Larger numbers of steps or evanescent modes give indistinguishable results in figure 3. Results of the benchmark model are in good agreement with the measurements of Davies & Heathershaw (1984), except when reflection over the bars is comparable with reflection over the beach, not included in

https://doi.org/10.1017/S0022112006004484 Published online by Cambridge University Press

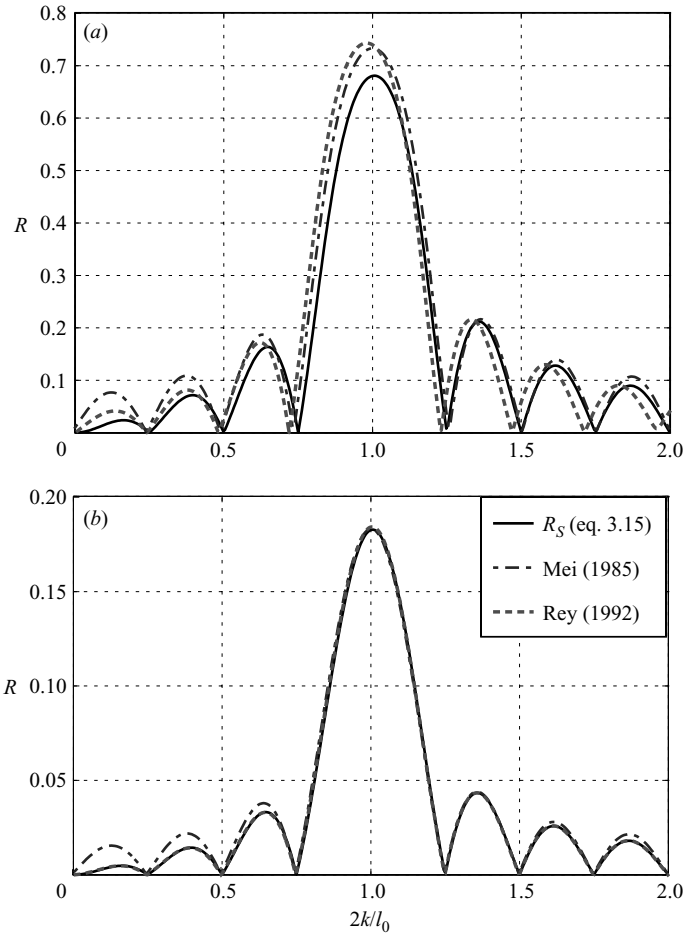


FIGURE 3. Reflection coefficients for the wave amplitudes for $U=0$, $H=0.156$ m, $l_0=2\pi$, $n=4$. (*a*) $b=0.05$ m so that $\eta=b/H=0.32$, corresponding to one of the experiments of Davies & Heathershaw (1984); (*b*), $b=0.01$ m, so that $\eta=b/H=0.064$.

the model. An analytical expression R_{Mei} is given by Mei (1985), but it is an exact solution for $2k=l_0$ only. R for the present second-order theory is given by R_S (3.15).

The predicted analytical convergence of (3.19) with Mei's (1985) solution is illustrated on figure 3, and particularly 3(b). Results for $\eta=0.34$ and $m=4$ (figure 3*a*) are also given because Mei's (1985) solution and Rey's (1992) model have been shown to reproduce accurately the laboratory measurements of Davies & Heathershaw (1984) for this choice of bottom shape and mean water level. This convergence provides a verification that the first-order scattering term S_1 is different from Hara & Mei's (1987) energy transfer term, and only accounts for a small fraction of the reflection, a fraction that goes to zero as $\eta\to 0$.

For large bar amplitudes, such as $\eta=b/H=0.32$ (figure 3*a*), all theories with linearized bottom boundary conditions fail to capture the shift of the reflection pattern to lower wavenumbers. This effect is most pronounced at high wavenumbers and is due to the nonlinear nature of the dispersion relation with respect to the depth. For a given frequency the wavenumber k corresponding to the mean depth is shorter than the mean wavenumber $\widehat{k}$, which is the one satifying the resonance

https://doi.org/10.1017/S0022112006004484 Published online by Cambridge University Press

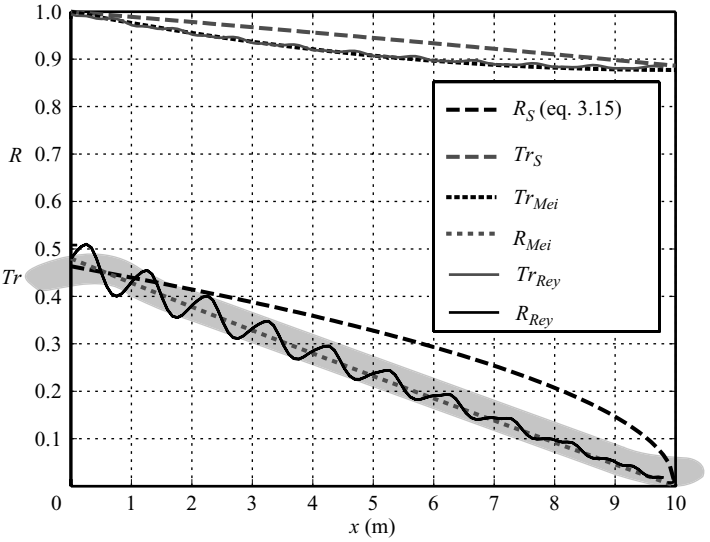


FIGURE 4. Spatial evolution of the incident and reflected wave amplitudes represented by transmission (Tr) and reflection (R) coefficients, in the case $U=0$, $H=0.42\,\mathrm{m}$, $l_0=2\pi\,\mathrm{m}^{-1}$, $m=10$ bars, $b=5\,\mathrm{cm}$, $\eta=b/H=0.12$ and with a near-resonant wave period. This situation with $T=1.23\,\mathrm{s}$ corresponds to one of the experiments of Davies & Heathershaw (1984), and their measurements lie in the shaded area. The upper and lower sets of curves correspond to Tr and R respectively. Model results are shown for $T=1.22\,\mathrm{s}$ so that Mei's analytical result is an exact solution of his equations. Rey's model is used with three evanescent modes and twelve steps per bottom period. The amplitudes shown are those of the free waves only.

condition $\widehat{k}=l_0/2$ (Rey 1992). Away from resonance, and for $\eta\ll 1$, R_S provides a better approximation to R_{Rey} than Mei's approximate analytical solution (figure 3*b*).

Probably, the most important limitation of the Bragg scattering approximation is that it cannot resolve spatial variations of the wave properties on scales shorter than the bottom autocorrelation length, which, in the case of a sinusoidal bottom, is equal to the length L of the bar patch. This is illustrated in figure 4, with the spatial variation of the incident and reflected wave amplitudes for resonant waves over sinusoidal bars. The scattering source term predicts a linear spatial evolution of the energy, while it is the amplitude which is observed to evolve linearly in this case. The amplitude evolution equation and Rey's model are able to reproduce the observed spatial evolution of the amplitudes (higher-order corrections are generally needed for Mei's theory in non-resonant cases (Hara & Mei 1987)). Still, as predicted by Kreisel (1949) and MAHR, the overall reflection coefficient $R(x=0)$ is estimated well by R_S.

3.5. *Effects of currents*

A prominent feature of solutions with a current is the modification of the resonant condition from $k=k'$ and $l=2k$, to $\sigma'=\sigma+lU$ and $l=k+k'$, discussed in detail by Kirby (1988). This shift was verified in the laboratory by Magne, Rey & Ardhuin (2005*b*). The magnitude of the resonant peak is also greatly enhanced for waves against the current, owing to a general conservation of the action fluxes and the variation in the action transport velocity, from C_g+U for the incident waves, to C'_g-U for the reflected waves. Further, the modulation of the current and the surface elevation also introduce an additional scattering, via the M_c term in the coupling

https://doi.org/10.1017/S0022112006004484 Published online by Cambridge University Press

coefficient (2.46). Notation here assumes that $\boldsymbol{k}$ is in the direction of the current and $\boldsymbol{k}'$ is opposite to the current. At resonance, in the limit $\eta \to 0$, the amplitude reflection coefficient R_S given by (3.15) converges to the reflection coefficient given by Kirby (1988). In our notation, he obtained

$$R_{\text{Kirby}} = \left[\frac{\sigma'(Cg+U)}{\sigma(Cg'-U)}\right]^{1/2} \tanh(QL), \tag{3.21}$$

with

$$Q = \frac{\Omega_c \omega}{[\sigma\sigma'(Cg+U)(Cg'-U)]^{1/2}} \tag{3.22}$$

and $\Omega_c = -M(k,k')b/[4\omega F^B(k-k')]$. Our amplitude reflection coefficient R_S is estimated with the approximation $\mathrm{e}^{q\boldsymbol{Q}L} = (\boldsymbol{I}+q\boldsymbol{Q})L + O((qL)^2)$, so that, to first order in qL,

$$R_S \approx \left[\frac{\sigma' C_g C_g' qL}{\sigma}\right]^{1/2}. \tag{3.23}$$

Substituting the analytical expression (3.4) in (3.11) yields

$$R_S \approx \frac{bLM(k,k')}{4[\sigma^2(C_g'-U)^2]^{1/2}}, \tag{3.24}$$

which is identical to (3.21) at first order in qL.

For finite values of qL, the reflection coefficient (3.15) corresponding to the solution of (3.9) is obtained by calculating the appropriate matrix exponential. Anticipating oceanographic conditions with a water depth of 30 m, a strong 3 m s^{-1} current corresponds to a Froude number of 0.17 only. For this low value of Fr in the context of Davies & Heathershaw's (1984) laboratory experiments, the convergence of the present theory and that of Kirby (1988) is illustrated in figure 5. The reflection coefficient is greatly increased for following currents due to the general conservation of the wave action flux. In that case R is enhanced by the factor $\{\sigma(Cg+U)/[\sigma'(Cg'-U)]\}^{1/2}$. The overall increase in R for following waves amounts to about 60 % at $Fr = 0.17$, for the laboratory sinusoidal bars of Davies & Heathershaw (1984) shown in figure 3, with a reflected wave energy multiplied by a factor 2.5 compared to the case without current. For this mild current the contribution M_c of the current fluctuation to the coupling coefficient M is small, with a maximum increase of 16 % in the action reflection coefficent, and 8 % for the wave amplitude. However, for larger Froude numbers, this additional scattering may become significant as illustrated by figure 6.

For $m = 4$ sinusoidal bars, the energy reflection coefficient was found to be within 10 % of the exact solution for over 90 % of the wavenumber range shown in figure 3, for $\eta < 0.1$ and $Fr = 0$, and this conclusion is expected to hold for $Fr < 0.2$, given the agreement with Kirby's (1988) approximate solution. This accuracy is twice as good as that found by MAHR for a rectangular step with $Fr = 0$.

The present method has the advantage of a large saving in computing power. It is also adapted well for natural seabeds, for which continuous bathymetric coverage is only available in restricted areas, and thus only the statistical properties of the bottom topography are accessible, assuming homogeneity.

https://doi.org/10.1017/S0022112006004484 Published online by Cambridge University Press

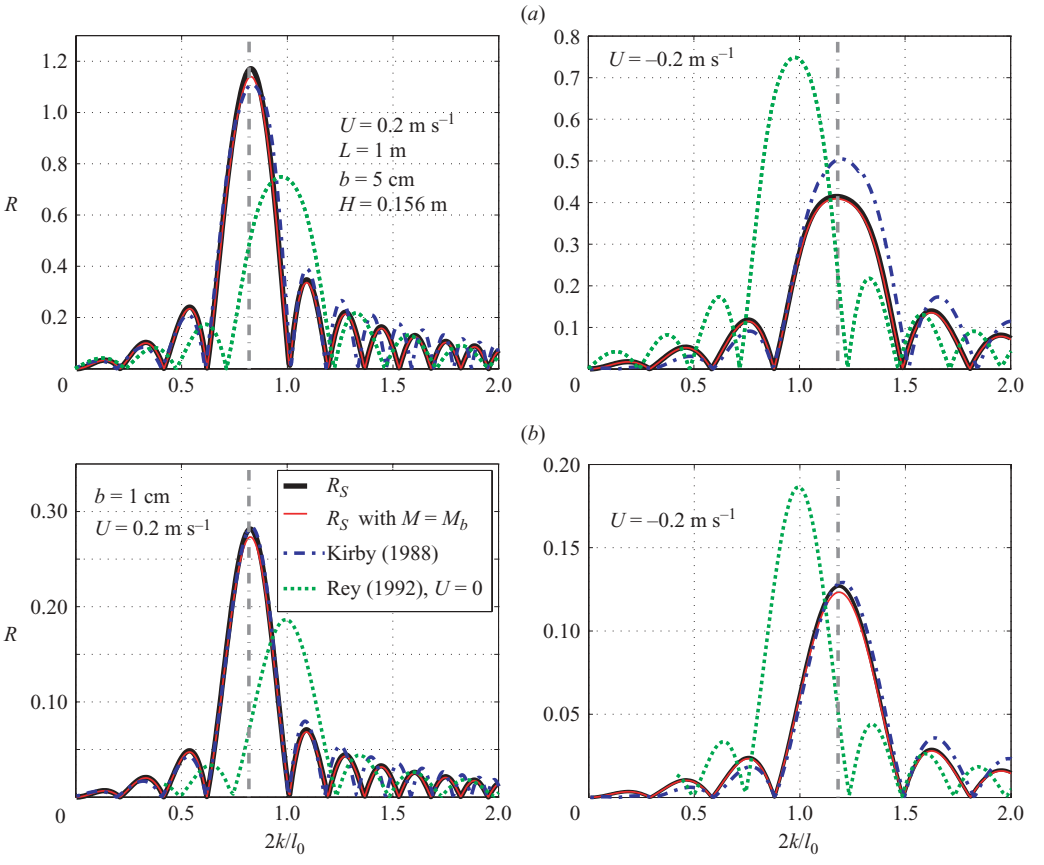


FIGURE 5. Amplitude reflection coefficients for monochromatic waves over sinusoidal bars for the same settings as in figure 3, with a following or opposing current of magnitude $U = 0.2\,\mathrm{m\,s^{-1}}$, and (*a*) $b/H = 0.32$, (*b*) $b/H = 0.064$. For reference the reflection coefficient without current, as given by the exact model of Rey (1995), is also shown. The position of the resonant wavenumber is indicated with the grey vertical dash-dotted line.

4. Evolution of waves over a three-dimensional random bottom

The scattering of waves with a continuous spectrum differs from the cases investigated so far owing to the coupling of wave components in all directions. Although a diffusion approximation may be feasible in cases of clear scale separation (e.g. Fabrikant & Raevsky 1994), this is generally not the case for wave–bottom scattering. An example bottom elevation map from the southern North Sea is shown in figure 7(*a*). Its spectrum is compared to North Carolina bottom spectra and the typical scales of waves that undergo significant scattering (figure 7*b*, *c*). For swells propagating from a distant storm with a fixed absolute frequency $\omega = \sigma + \boldsymbol{k}\cdot\boldsymbol{U}$, a change in the current modifies the angle of the scattered waves, or equivalently, waves scattered in a given direction correspond to reflections on different bottom undulations with widely different variances. This effect is illustrated in figure 7(*b*), and exaggerated by taking a mean water depth of 25 m instead of 35 m at mid-tide. Given a fixed primary wave of wavenumber $\boldsymbol{k}$ corresponding to a period 12.5 s, the current modifies the locus of the scattered wavenumbers $\boldsymbol{k}'$ that interact with $\boldsymbol{k}$.

https://doi.org/10.1017/S0022112006004484 Published online by Cambridge University Press

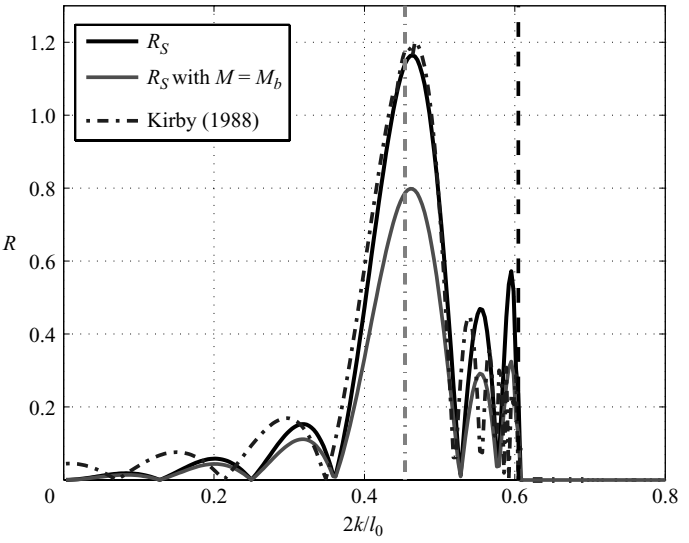


FIGURE 6. Amplitude reflection coefficients for monochromatic waves over sinusoidal bars for the same settings as in figures 3 and 4, $b/H = 0.064$, $b = 1$ cm, with a stronger following current of magnitude $U = 0.6$ m s^{-1}. The position of the resonant wavenumber is indicated with the grey vertical dash-dotted line. The vertical dashed line corresponds to the wavenumber for which $C_g' = U$. For larger wavenumbers the reflected waves propagate against the current but are advected downstream.

A simple account of the spectral evolution can be given for uniform conditions. The scattering source term is a linear function of the directional spectrum at a given value of the absolute frequency ω. We consider the wave action directional spectrum for a frequency f_0 and discretize it in N_a directions. This spectrum is thus a vector $\boldsymbol{A}$ in a space with N_a dimensions. The evolution of $\boldsymbol{A}$ given by (2.52) can be written in matrix form as $\mathrm{d}\boldsymbol{A}/\mathrm{d}t = \boldsymbol{S}\boldsymbol{A}$. $\boldsymbol{S}$ is a symmetric and positive square matrix, which can thus be diagonalized, giving N_a eigenvalues λ_n and corresponding eigenvectors $\boldsymbol{V}_n$, such that $\boldsymbol{S}\boldsymbol{V}_n = \lambda_n \boldsymbol{V}_n$. Thus the time evolution is easily obtained by a projection of $\boldsymbol{A}$ on the basis $\{\boldsymbol{V}_n, 1 \leqslant n \leqslant N_a\}$, giving a decomposition of $\boldsymbol{A}$ in elementary components. Each of these components of the directional spectrum decays exponentially in time, except for the isotropic part of the spectrum which remains constant because that eigenvector corresponds to $\lambda = 0$. The eigenvalues thus give interesting time scales for the evolution of the spectrum toward this isotropic state, with a half-lifetime of each eigenvector given by $-\ln 2/\lambda_n$.

Using the bottom spectrum shown in figure 7(*b*), numerical estimates of the eigenvalues are given in figure 8, with and without current, for 12.5 s waves in 35 m depth. Given the low Froude number ($Fr \approx 0.1$), the term M_c is neglected in the coupling coefficient. Results are shown for $N_a = 120$, corresponding to a directional resolution of 3°, and similar results were found for $N_a = 180$ and $N_a = 72$.

The shortest time scales (largest negative values of λ_n) correspond to directional spectra (eigenvectors) with strong local variations. These eigenvectors are thus associated with scattering at small oblique angles (forward-scattering). Only the last 10 eigenvalues have a rather broad support, corresponding to scattering at much larger angles. Also, the strongest scattering corresponds to a half-lifetime of 4600 s, and mostly affects waves from the north-west or south-east, i.e. propagating in a direction along the sandwave crests. The evolution time scale for waves from the north-east

https://doi.org/10.1017/S0022112006004484 Published online by Cambridge University Press

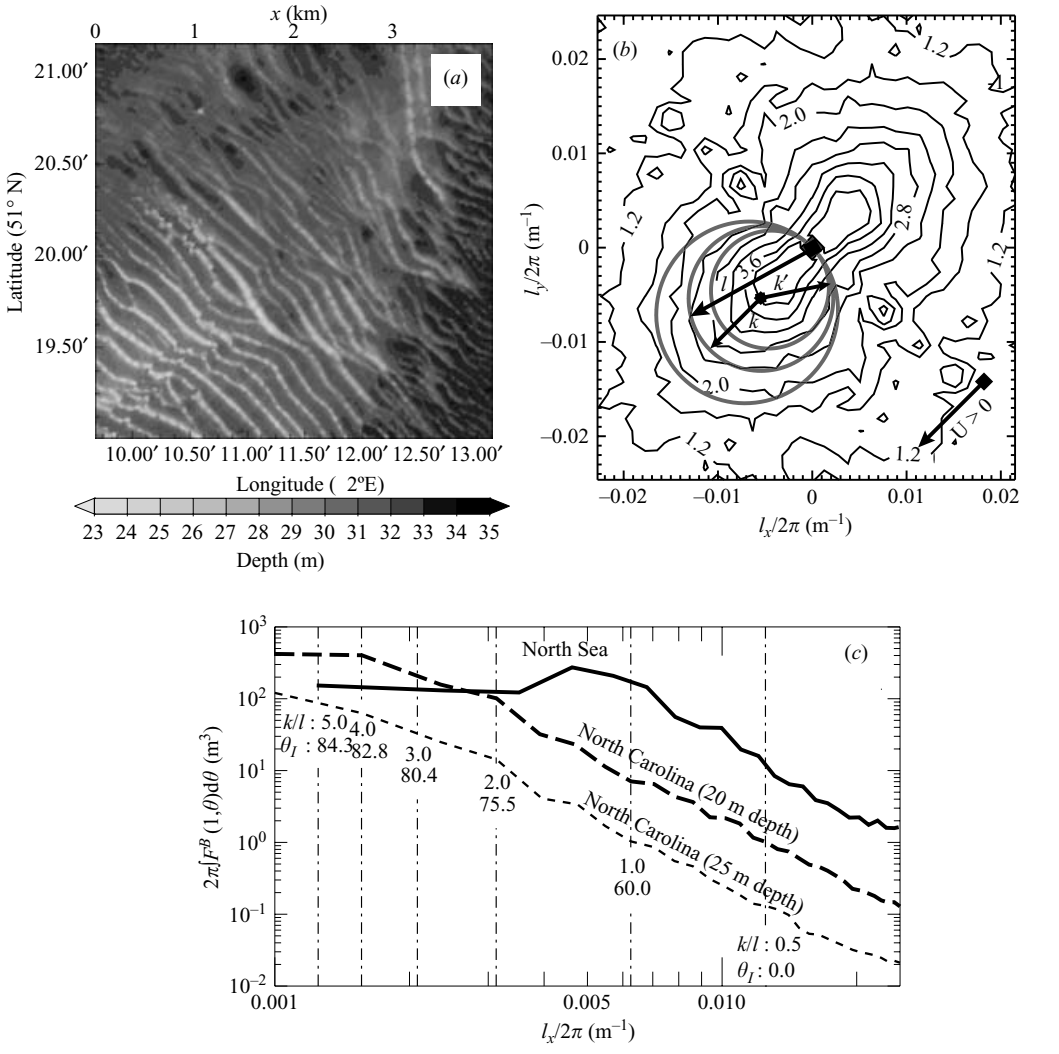


FIGURE 7. (*a*) High-resolution bathymetry of a sandwave field in the southern North Sea with depths relative to chart datum, and (*b*) corresponding bottom elevation spectrum with contour values representing $\log_{10}(4\pi^2 F^B)$. The locus of the interacting bottom and surface wave components are indicated for a 12.5 s waves from the north-east in 25 m depth, with $U = 0$ (middle circle), $U = 2\,\mathrm{m\,s^{-1}}$ (smaller ellipse), and $U = -2\,\mathrm{m\,s^{-1}}$ (larger ellipse), U is positive from the north-east. (*c*) Direction-integrated bottom variance spectra from the North Carolina shelf and the southern North Sea. Vertical lines indicate k/l ratios and incident resonant directions θ_I, assuming an incident wave field of 12.5 s period in 25 m depth and bedforms parallel to the y-axis. For such bedforms, the angle between incident and scattered waves is $180^\circ - 2\theta_I$.

or south-west is about three times larger. Eigenvectors corresponding to the smallest non-zero eigenvalues (here a half-life over 6 hours) have amplitudes of opposite signs for components travelling in opposite directions across the sandwaves and thus correspond to back-scattering, which is weaker than the forward-scattering. Without current the scattering pattern is centrally symmetric owing to the central symmetry of the bottom spectrum. A current breaks this symmetry with stronger scattering for

https://doi.org/10.1017/S0022112006004484 Published online by Cambridge University Press

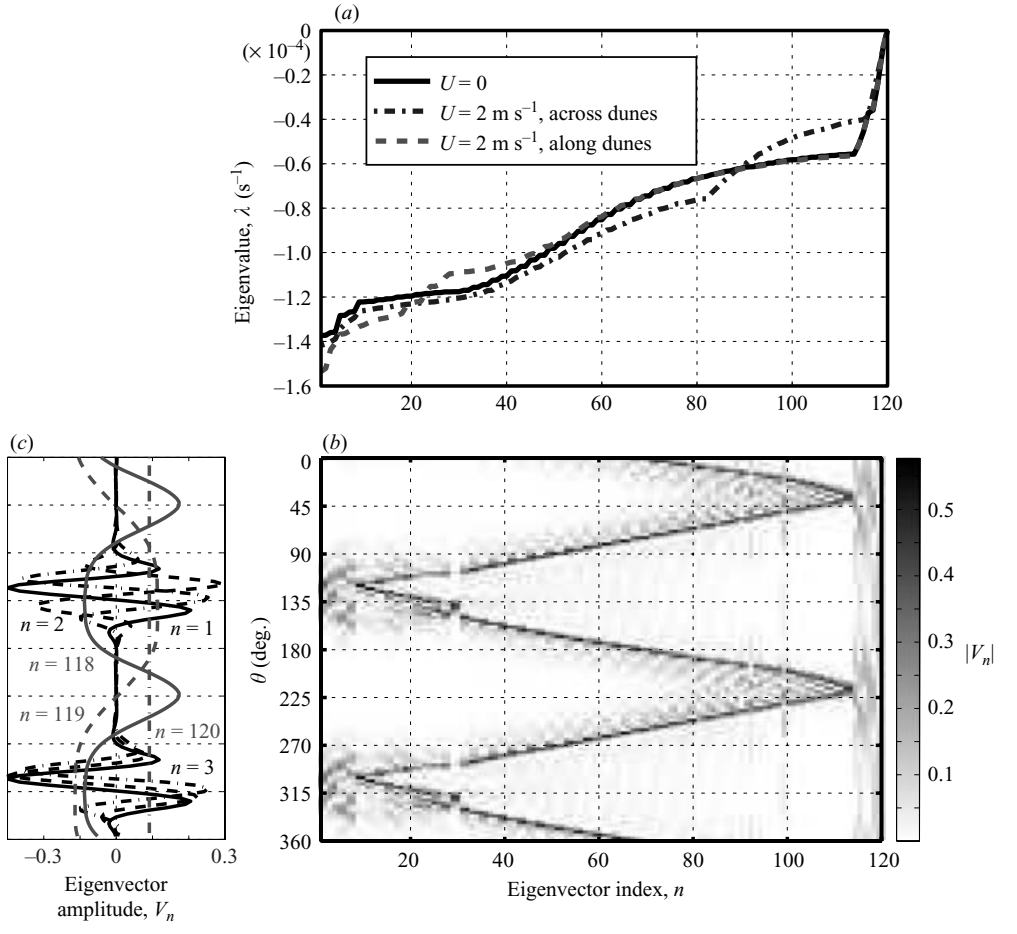


FIGURE 8. Eigenvalues ordered by magnitude for $U=0$, and $U=2\,\mathrm{m\,s^{-1}}$ with two current directions (a), and corresponding absolute values of the eigenvector matrix (b) for $U=0$, $f_0=0.08$ Hz, and $H=35\,\mathrm{m}$. The first three and last three eigenvectors are shown in more detail in (c). Directions use the trigonometric convention so that 0° and 90° correspond to waves from the West and South, respectively.

waves propagating downstream (although the eigenvalues do not change much, the corresponding eigenvectors are very different).

In all cases, a standard diffusion approximation (e.g. $S_{\mathrm{bscat}}(\omega,\theta)\simeq D_\omega\partial^2 A(\omega,\theta)/\partial\theta^2$), appears inappropriate in the case presented here. Indeed, the scattering effect may be compared to a diffusion operator in θ-space for which the eigenvectors are sines and cosines such as $\boldsymbol{A}_n=(\cos ni\theta_r)_{1\leqslant i\leqslant N_a}$ with $\theta_r=2\pi/N_a$. Although the eigenvalues are proportional to n^2 for diffusion, the strength of the scattering for directional spectra such as $\boldsymbol{A}_n$ is roughly constant here, for $n<N_a/8$.

However, practical situations are not horizontally uniform, and correspond to quasi-stationary conditions with spatial gradients in at least one dimension. As an example, a calculation with the same bottom spectrum was performed with a one-dimensional model configuration. For waves of period 12.5 s in 35 m depth, an initial directional spreading of 12° increased up to 35° after 100 km of propagation and 12 hours of integration. This maximum value was found for waves propagating along the

https://doi.org/10.1017/S0022112006004484 Published online by Cambridge University Press

sandwave crests, and was weakly modulated by the current. The strongest effect of currents is a change of reflected wave energy for waves propagating across the sandwaves. That effect is identical to the change in the magnitude of the reflection coefficients due to the conservation of the wave action flux and shown on figure 5.

5. Conclusion and perspectives

The effect of a uniform current on the scattering of random surface gravity waves was investigated theoretically, extending the derivations of Ardhuin & Herbers (2002). Wave scattering results from both water depth variations on the scale of the surface gravity wave wavelength and current and mean free-surface inhomogeneities induced by the bottom topography. All these effects are represented by a scattering source term $S_{\mathrm{bscat}}(\boldsymbol{k})$ in the spectral action balance equation. That term is the rate of exchange of wave action between all wave components $\boldsymbol{k}$ and $\boldsymbol{k}'$ that have the same absolute frequency. The exchange of action among any wave component pair $\boldsymbol{k}$ and $\boldsymbol{k}'$ is proportional to the bottom elevation spectrum at the wavenumber vector $\boldsymbol{l} = \boldsymbol{k} - \boldsymbol{k}'$, which is characteristic of Bragg scattering. The spectral integral of the corresponding wave pseudo-momentum source term $\boldsymbol{k}S_{\mathrm{bscat}}$ gives a recoil force exerted by the bottom on the water column, in addition to the hydrostatic pressure force.

MARH have proved that the source term is applicable to non-random topography, and is accurate in the limit of small bottom amplitudes, a result that can also be inferred from the work of Kreisel (1949). It is further found here that monochromatic wave results are recovered by taking the limit to narrow incident and reflected wave spectra. In the absence of current, and for a finite sinusoidal bottom and monochromatic waves, the reflection coefficients given by the source term converge to Mei's (1985) results in the limit of small bottom amplitudes. The range of maximum reflection and the side lobe pattern of the reflection coefficient as a function of the incident wavenumber is thus a direct consequence of the shape of the bottom spectrum in that case. With this point of view, there is resonance at all wavenumbers but its strength is proportional to the bottom elevation variance at the corresponding scale. In the presence of a current, reflections converge in the same manner to the more general theory of Kirby (1988). In two dimensions, the main effect of a current is an enhancement of reflected wave amplitudes when the incident waves propagate with the current, owing to conservation of the wave action flux, and a Doppler-like shift of the resonant wave frequencies that undergo maximum reflection. The two-scale approximation was found to hold very well, even for a relatively fast evolution of the wave amplitudes over two wavelengths (e.g. figure 3). However, the source term does not give a good representation of the spatial evolution of the wave field on scales shorter than the bottom correlation length, nor can it give reasonable results when another wavetrain propagates from beyond the bars. In that case, a lower-order source term must be considered, and a closed action balance cannot be obtained since that extra term depends on the phase relationship between the incident waves, reflected waves and bottom undulations.

Over natural topographies, the bottom typically de-correlates over scales shorter than the scattering-induced attenuation scales, so that a modification of the reflection due to a phase locking of the incident and reflected waves with the bottom can be neglected. In three dimensions and over the shallow areas of the southern North Sea, where large sandwaves are found with strong tidal currents, wave scattering is expected to be significant, and influenced by currents. This effect probably accounts for part of the observed attenuation of swells in that region (Weber 1991). A realistic application of the present theory to this area will be described elsewhere.

https://doi.org/10.1017/S0022112006004484 Published online by Cambridge University Press

The representation of wave scattering with a source term in the wave action balance equation is well suited to engineering and scientific investigations of large-scale wave evolution. The approximation given by the present theory is expected to be accurate in many conditions of interest. The alternative use of phase-resolving elliptic refraction–diffraction models (e.g. Belibassakis, Athanassoulis & Gerostathis 2001) is much more expensive in terms of computer resources, owing to the necessity to resolve the wave phase, and the ellipticity of the problem when back-scattering occurs.

For applications to rotational currents, the mean current U should be regarded as the wave advection velocity (Andrews & McIntyre 1978, see Kirby & Chen 1989 for approximate expressions). A detailed derivation including scattering in the presence of general rotational current fluctuations should be the next logical extension of the present theory. Such work could also provide an extension to intermediate depth of Rayevskiy's (1983) theory for the scattering of waves over random currents. Finally, non-homogeneities in the bottom spectrum will probably have to be addressed owing the sharp decrease of the wave–bottom coupling coefficient with water depth, and the generally higher bottom elevation variances in the shallower parts of the sea floor. Our limited bathymetric surveys show that sandwaves are modulated by sand dunes, very much like short water waves are modulated by long waves.

R. M. was supported by a joint grant from CNRS and DGA, and performed the derivations in § 2 and Appendix B. These were slightly corrected by F. A. who added the remainder of the paper. Bathymetric data were acquired by the French Hydrographic and Oceanographic Service (SHOM). Discussions with Michael McIntyre, Kostas Belibassakis, Vincent Rey, and Thierry Garlan are gratefully acknowledged. The effect of current modulations was investigated following remarks made by anonymous reviewers, without whom the present paper would have been limited to small Froude numbers.

Appendix A. Harmonic oscillator equation for the first-order potential

The harmonic oscillator equation (2.31) can be written as a linear superposition of equations of the type

$$\frac{\mathrm{d}^2 f_1}{\mathrm{d}t^2} + \omega^2 f_1 = \mathrm{e}^{\mathrm{i}\omega' t}. \tag{A 1}$$

In order to specify a unique solution to (A 1), initial conditions must be prescribed. In the limit of large propagation distances, the initial conditions contribute a negligible non-secular term to the solution. Following Hasselmann (1962), we choose $f_1(0) = 0$ and $\mathrm{d}f_1/\mathrm{d}t(0) = 0$, giving

$$f_1(\omega, \omega'; t) = \frac{\mathrm{e}^{\mathrm{i}\omega' t} - \mathrm{e}^{\mathrm{i}\omega t} + i(\omega - \omega')\sin(\omega t)/\omega}{\omega^2 - \omega'^2} \qquad \text{for} \qquad \omega'^2 \neq \omega^2, \tag{A 2}$$

$$f_1(\omega, \omega'; t) = \frac{t\mathrm{e}^{\mathrm{i}\omega' t}}{2i\omega'} - \frac{\sin'(\omega t)}{2i\omega'\omega} \qquad \text{for} \qquad \omega' = \pm\omega. \tag{A 3}$$

Appendix B. Second-order potential

In order to estimate all terms that contribute to N_2, the second-order potential ϕ_2 must be obtained. It is a solution of

$$\nabla^2\phi_2 + \frac{\partial^2\phi_2}{\partial z^2} = 0 \qquad \text{for} \qquad -H \leqslant z \leqslant 0. \tag{B 1}$$

https://doi.org/10.1017/S0022112006004484 Published online by Cambridge University Press

Because odd vertical derivatives of ϕ_0 are zero at $z=-H$, one has

$$\frac{\partial\phi_2}{\partial z} = -h\frac{\partial^2\phi_1}{\partial z^2} + \nabla\phi_1\cdot\nabla h \qquad \text{at} \qquad z=-H, \tag{B 2}$$

and

$$\frac{\partial^2\phi_2}{\partial t^2} + g\frac{\partial\phi_2}{\partial z} = \mathrm{i}\sum_{\boldsymbol{k},s} 2s\sigma\frac{\partial\Phi^s_{0,\boldsymbol{k}}}{\partial t}\mathrm{e}^{\mathrm{i}(\boldsymbol{k}\cdot\boldsymbol{x}-s\omega t)} + \text{I–VIII} + NL_2 \qquad \text{at} \qquad z=0. \tag{B 3}$$

The terms I–VIII are those in (2.22) with ϕ_0, ζ_0, ϕ_1, ζ_1 replaced by $(\phi_1-\phi_{1c})$, $(\zeta_1-\zeta_{1c})$, ϕ_2 and ζ_2, respectively. All other nonlinear terms have been grouped in NL_2. In order to yield contributions to the second-order action $N_{2,0}$, terms must correlate with ϕ_0 to give second-order terms in η with non-zero means. For zeroth-order components with random phases, inspection shows that NL_2 does not contribute to $N_{2,0}$ and will thus be neglected.

The solution ϕ_2 is given by

$$\phi_2 = \phi_2^{\mathrm{ns}} + \sum_{\boldsymbol{k},s}\left[\frac{\cosh(k(z+H))}{\cosh(kH)}\Phi^s_{2,\boldsymbol{k}}(t) + \frac{\sinh(k(z+H))}{\cosh(kH)}\Phi^{\mathrm{si},s}_{2,\boldsymbol{k}}(t)\right]\mathrm{e}^{\mathrm{i}\boldsymbol{k}\cdot\boldsymbol{x}}. \tag{B 4}$$

The non-stationarity term ϕ_2^{ns} leads to the action evolution term (2.37), now assuming $\gamma\approx\eta^2$. Following the method used at first order, substitution of (B 4) in the bottom boundary condition (B 2) leads to

$$\Phi^{\mathrm{si},s}_{2,\boldsymbol{k}}(t) = -\sum_{\boldsymbol{k}'}\frac{\boldsymbol{k}'\cdot\boldsymbol{k}}{k}\frac{\cosh(kH)}{\cosh(k'H)}\Phi^s_{1,\boldsymbol{k}'}(t)G_{\boldsymbol{k}-\boldsymbol{k}'}\mathrm{e}^{\mathrm{i}\boldsymbol{l}\cdot\boldsymbol{U}t}. \tag{B 5}$$

Substituting ϕ_1 (2.29) in the surface boundary condition (B 3) yields

$$\left(\frac{\mathrm{d}^2}{\mathrm{d}t^2}+\sigma^2\right)\Phi^s_{2,\boldsymbol{k}}(t) = -gk\Phi^{\mathrm{si},s}_{2,\boldsymbol{k}} - \tanh(kH)\frac{\partial^2\Phi^{\mathrm{si},s}_{2,\boldsymbol{k}}}{\partial t^2} + \text{I–VIII}, \tag{B 6}$$

and conserving only the resonant terms of $\Phi^s_{1,\boldsymbol{k}'}$, one obtains

$$\frac{\partial^2\Phi^{\mathrm{si},s}_{2,\boldsymbol{k}}}{\partial t^2} = -\sum_{\boldsymbol{k}',\boldsymbol{k}''}\frac{\boldsymbol{k}'\cdot\boldsymbol{k}}{k}\frac{\cosh(kH)}{\cosh(k'H)}M(\boldsymbol{k}',\boldsymbol{k}'')G_{\boldsymbol{k}-\boldsymbol{k}'}G_{\boldsymbol{k}'-\boldsymbol{k}''}\Phi_{0,\boldsymbol{k}''}\frac{\partial^2}{\partial t^2}(f_1(\sigma',\boldsymbol{l}'\cdot\boldsymbol{U}-s\sigma'')\mathrm{e}^{\mathrm{i}\boldsymbol{l}\cdot\boldsymbol{U}t}), \tag{B 7}$$

with $\boldsymbol{l}'=(\boldsymbol{k}''-\boldsymbol{k}')\cdot\boldsymbol{U}$. In order to simplify the algebra we assume that the zeroth-order waves are random, with no correlation between $\Phi^s_{0,\boldsymbol{k}}$ and $\Phi^{s''}_{0,\boldsymbol{k}''}$ unless $\boldsymbol{k}=\pm\boldsymbol{k}''$ and $s=\pm s''$. Thus the only terms contributing to $N_{2,0}$ must satisfy $\boldsymbol{k}''=\boldsymbol{k}$. Only those terms are now written explicitly, the others being grouped in '…'. The amplitude $\Phi^+_{2,\boldsymbol{k}}$ satisfies the following forced harmonic oscillator equation:

$$\left(\frac{\partial^2}{\partial t^2}+\sigma^2\right)\Phi^+_{2,\boldsymbol{k}}(t) = \sum_{\boldsymbol{k}'}M^2(\boldsymbol{k},\boldsymbol{k}')|G_{\boldsymbol{k}-\boldsymbol{k}'}|^2\Phi_{1,\boldsymbol{k}''}f_1(\sigma',-\sigma-\boldsymbol{l}\cdot\boldsymbol{U})\mathrm{e}^{\mathrm{i}\boldsymbol{l}\cdot\boldsymbol{U}t}+\cdots. \tag{B 8}$$

This is a sum of equations of the form

$$\left(\frac{\mathrm{d}^2}{\mathrm{d}t^2}+\sigma^2\right)f_2 = f_1(\sigma',\boldsymbol{l}\cdot\boldsymbol{U}-\sigma;t)\mathrm{e}^{\mathrm{i}\boldsymbol{l}\cdot\boldsymbol{U}t}. \tag{B 9}$$

The solution f_2 may be written as

$$f_2 = f_{2,a}+f_{2,b}, \tag{B 10}$$

https://doi.org/10.1017/S0022112006004484 Published online by Cambridge University Press

where

$$f_{2,a} = -\frac{t\mathrm{e}^{-\mathrm{i}\sigma t} - \sin(\sigma t)/\sigma}{2\mathrm{i}\sigma\,[\sigma'^2 - (\boldsymbol{l}\cdot\boldsymbol{U}+\sigma)^2]}, \tag{B 11}$$

$$f_{2,b} = -\frac{1}{2\sigma'\,[\sigma' - (\boldsymbol{l}\cdot\boldsymbol{U}+\sigma)]} \times \left[\frac{\mathrm{e}^{-\mathrm{i}(\sigma'-\boldsymbol{l}\cdot\boldsymbol{U})t}}{\sigma^2 - (\sigma'-\boldsymbol{l}\cdot\boldsymbol{U})^2} - \frac{1}{2\sigma}\left(\frac{\mathrm{e}^{\mathrm{i}\sigma t}}{\sigma + (\sigma'-\boldsymbol{l}\cdot\boldsymbol{U})} + \frac{\mathrm{e}^{-\mathrm{i}\sigma t}}{\sigma - (\sigma'-\boldsymbol{l}\cdot\boldsymbol{U})}\right)\right]. \tag{B 12}$$

Taking the correlation with $\Phi^s_{0,-\boldsymbol{k}}$, all terms are zero except for $\boldsymbol{k}''=\boldsymbol{k}$, which removes the '…' terms, so that (B 8) becomes

$$\frac{\langle \Phi^+_{2,\boldsymbol{k}}\Phi^-_{0,-\boldsymbol{k}}\rangle}{\Delta\boldsymbol{k}} = \sum_{\boldsymbol{k}'} M^2(\boldsymbol{k},\boldsymbol{k}')\frac{\langle|G_{\boldsymbol{k}-\boldsymbol{k}'}|^2\rangle}{\Delta\boldsymbol{k}}\frac{\langle \Phi^+_{0,\boldsymbol{k}}\Phi^-_{0,-\boldsymbol{k}}\rangle}{\Delta\boldsymbol{k}}\langle f_2\mathrm{e}^{\mathrm{i}\sigma t}\rangle\Delta\boldsymbol{k}, \tag{B 13}$$

with

$$\langle f_2\mathrm{e}^{\mathrm{i}\sigma t}\rangle = \frac{\pi t}{8\sigma\sigma'}\{\delta[\sigma' - (\sigma - \boldsymbol{l}\cdot\boldsymbol{U})] + O(1)\}. \tag{B 14}$$

Taking the limit $\Delta\boldsymbol{k}\to 0$, and neglecting $O(1)$ terms yields

$$F^{\Phi}_{2,0}(t,\boldsymbol{k}) = -\int_{\boldsymbol{k}'}\frac{\pi t}{4\sigma}M^2(\boldsymbol{k},\boldsymbol{k}')F^B(\boldsymbol{k}-\boldsymbol{k}')\frac{F^{\Phi}_{0,0}(\boldsymbol{k})}{\sigma'}\delta(\omega'-\omega)\,\mathrm{d}\boldsymbol{k}'. \tag{B 15}$$

Changing the spectral coordinates from $\boldsymbol{k}'$ to (ω',θ') allows a simple removal of the singularity,

$$F^{\Phi}_{2,0}(t,\boldsymbol{k}) = -\int_0^{2\pi}\frac{\pi t}{4\sigma}M^2(\boldsymbol{k},\boldsymbol{k}')F^B(\boldsymbol{k}-\boldsymbol{k}')\frac{F^{\Phi}_{0,0}(\boldsymbol{k})}{\sigma'}\frac{k'}{Cg' + \boldsymbol{k}'\cdot\boldsymbol{U}/k'}\mathrm{d}\theta'. \tag{B 16}$$

Appendix C. Resonant wavenumber configuration for $U \ll C_g$

Under the assumption $U \ll C_g$, and for a current in the x direction, the resonant conditions

$$\sigma' - \sigma = l_x U \tag{C 1}$$

yields the following Taylor expansion to first order in $\sigma'-\sigma$:

$$k' - k = (k'_x - k_x)\frac{U}{C_g} + O\left[k\left(\frac{U}{C_g}\right)^2\right]. \tag{C 2}$$

This may be written as

$$k' \simeq \frac{P}{1 + e\cos\theta'}. \tag{C 3}$$

This is the parametric equation of an ellipse (if $e<1$) in polar coordinates (k',θ') with one focus at the origin, and semi-major axis a, semi-minor axis b, half the foci distance c, and eccentricity e, with $P = k + U/C_g k\cos\theta = b^2/a$, and $e = U/C_g = c/a$. The interaction between a surface wave with wavenumber $\boldsymbol{k}'$ and a bottom component with wavenumber $\boldsymbol{l}$ excites a surface wave with the sum wavenumber $\boldsymbol{k}=\boldsymbol{k}'+\boldsymbol{l}$. For a fixed $\boldsymbol{k}$ and current U, in the limit of $U \ll C_g$ the resonant $\boldsymbol{k}'$ and $\boldsymbol{l}$ follow ellipses described by their polar equation (C 3), which reduce to circles for $U=0$. In the shallow water limit (C 3) is exact, and the locus of the resonant wavenumbers $\boldsymbol{k}'$ is exactly an ellipse for $Fr<1$ and becomes a hyperbola for $Fr>1$.

https://doi.org/10.1017/S0022112006004484 Published online by Cambridge University Press

REFERENCES

Andrews, D. G. & McIntyre, M. E. 1978 On wave action and its relatives. *J. Fluid Mech.* **89**, 647–664, and corrigendum: vol. 95, p. 796.

Annenkov, S. Y. & Shrira, V. I. 2006 A note on Hasselmann's energy-transfer model. *J. Fluid Mech.* **561**, 181–207.

Ardhuin, F. & Herbers, T. H. C. 2002 Bragg scattering of random surface gravity waves by irregular sea bed topography. *J. Fluid Mech.* **451**, 1–33.

Ardhuin, F., Herbers, T. H. C., Jessen, P. F. & O'Reilly, W. C. 2003*a* Swell transformation across the continental shelf. part II: validation of a spectral energy balance equation. *J. Phys. Oceanogr.* **33**, 1940–1953.

Ardhuin, F., O'Reilly, W. C., Herbers, T. H. C. & Jessen, P. F. 2003*b* Swell transformation across the continental shelf. part I: Attenuation and directional broadening. *J. Phys. Oceanogr.* **33**, 1921–1939.

Bal, G. & Chou, T. 2002 Capillary-gravity wave transport over spatially random drift. *Wave Motion* **35**, 107–124.

Belibassakis, K. A., Athanassoulis, G. A. & Gerostathis, T. P. 2001 A coupled-mode model for the refraction-diffraction of linear waves over steep three-dimensional bathymetry. *Appl. Ocean Res.* **23**, 319–336.

Belzons, M., Guazzelli, E. & Parodi, O. 1988 Gravity waves on a rough bottom: experimental evidence of one-dimensional localization. *J. Fluid Mech.* **186**, 539–558.

Benney, D. J. & Saffman, P. G. 1966 Nonlinear interactions of random waves in a dispersive medium. *Proc. R. Soc. Lond.* A **289**, 301–380.

Dalrymple, R., Knight, R. J. & Lambiase, J. J. 1978 Bedforms and their hydraulic stability relationships in a tidal environment, bay of Fundy, Canada. *Nature* **275**, 100–104.

Davies, A. G. & Heathershaw, A. D. 1984 Surface-wave propagation over sinusoidally varying topography. *J. Fluid Mech.* **144**, 419–443.

Elfouhaily, T. M. & Guérin, C.-A. 2004 A critical survey of approximate scattering wave theories from random rough surfaces. *Waves in Random Media* **14**, 1–40.

Elter, J. F. & Molyneux, J. E. 1972 The long-distance propagation of shallow water waves over an ocean of random depth. *J. Fluid Mech.* **53**, 1–15.

Fabrikant, A. L. & Raevsky, M. A. 1994 The influence of drift flow turbulence on surface gravity wave propagation. *J. Fluid Mech.* **262**, 141–156.

Guazzelli, E., Rey, V. & Belzons, M. 1992 Higher-order Bragg reflection of gravity surface waves by periodic beds. *J. Fluid Mech.* **245**, 301–317.

Hara, T. 1986 Resonant reflection of water waves by periodic sandbars. Master's thesis, Department of Civil Engineering, University of Tokyo, Japan.

Hara, T. & Mei, C. C. 1987 Bragg scattering of surface waves by periodic bars: theory and experiment. *J. Fluid Mech.* **178**, 221–241.

Hasselmann, K. 1962 On the non-linear energy transfer in a gravity wave spectrum, part 1: general theory. *J. Fluid Mech.* **12**, 481–501.

Hasselmann, K. 1966 Feynman diagrams and interaction rules of wave-wave scattering processes. *Rev. Geophys.* **4**, 1–32.

Heathershaw, A. D. 1982 Seabed-wave resonance and sand bar growth. *Nature* **296**, 343–345.

Herbers, T. H. C., Orzech, M., Elgar, S. & Guza, R. T. 2003 Shoaling transformation of wave-frequency directional spectra. *J. Geophys. Res.* **108** (C1), 3013, doi:10.1029/2001JC001304.

Idier, D., Erhold, A. & Garlan, T. 2002 Morphodynamique d'une dune sous-marine du détroit du Pas de Calais. *C. R. Géosci.* **334**, 1079–1085.

Janssen, T. T., Herbers, T. H. C. & Battjes, J. A. 2006 Generalized evolution equation for nonlinear surface gravity waves over two-dimensional topography. *J. Fluid Mech.* **552**, 393–418.

Kirby, J. T. 1986 A general wave equation for waves over rippled beds. *J. Fluid Mech.* **162**, 171–186.

Kirby, J. T. 1988 Current effects on resonant reflection of surface water waves by sand bars. *J. Fluid Mech.* **186**, 501–520.

Kirby, J. T. & Chen, T.-M. 1989 Surface waves on vertically sheared flows: approximate dispersion relations. *J. Geophys. Res.* **94** (C1), 1013–1027.

Kreisel, G. 1949 Surface waves. *Q. J. Appl. Maths* **7**, 21–44.

https://doi.org/10.1017/S0022112006004484 Published online by Cambridge University Press

Longuet-Higgins, M. S. 1950 A theory of the origin of microseisms. *Proc. R. Soc. Lond.* A **243**, 1–35.

Longuet-Higgins, M. S. 1967 On the wave-induced difference in mean sea level between the two sides of a submerged breakwater. *J. Mar. Res.* **25**, 148–153.

Magne, R., Ardhuin, F., Rey, V. & Herbers, T. H. C. 2005*a* Topographical scattering of waves: spectral approach. *J. Waterway, Port Coast. Ocean Engng* **131**, 311–320.

Magne, R., Rey, V. & Ardhuin, F. 2005*b* Measurement of wave scattering by topography in the presence of currents. *Phys. Fluids* **17**, 126601.

Mei, C. C. 1985 Resonant reflection of surface water waves by periodic sandbars. *J. Fluid Mech.* **152**, 315–335.

Miles, J. 1981 Oblique surface-wave diffraction by a cylindrical obstacle. *Dyn. Atmos. Oceans* **6**, 121–123.

Onorato, M., Osborne, A. R., Serio, M., Cavaleri, L., Brandini, C. & Stansberg, C. T. 2005 Observation of strongly non-gaussian statistics for random sea surface gravity waves in wave flume experiments. *Phys. Rev.* E **70**, 067302.

Phillips, O. M. 1977 *The Dynamics of the Upper Ocean*. Cambridge University Press.

Pihl, J., Mei, C. C. & Hancock, M. 2002 Surface gravity waves over a two-dimensional random seabed. *Phys. Rev.* E **66**, 016611.

Priestley, M. B. 1981 *Spectral Analysis and Time Series*. Academic.

Rayevskiy, M. A. 1983 On the propagation of gravity waves in randomly inhomogeneous nonstrady-state currents. *Izv. Atmos. Ocean. Phys.* **19** (6), 475–479.

Rayleigh, Lord 1896 *The Theory of Sound*, 3rd edn. Macmillan.

Rey, V. 1992 Propagation and local behaviour of normally incident gravity waves over varying topography. *Eur. J. Mech.* B/*Fluids* **11**, 213–232.

Ryzhik, L., Papanicolaou, G. & Keller, J. B. 1996 Transport equations for elastic and other waves in random media. *Wave Motion* **24**, 327–370, and corrigendum: vol. 95, p. 796.

Watson, K. M. & West, B. J. 1975 A transport-equation description of nonlinear ocean surface wave interactions. *J. Fluid Mech.* **70**, 815–826.

Weber, N. 1991 Bottom friction for wind sea and swell in extreme depth-limited situations. *J. Phys. Oceanogr.* **21**, 149–172.

Yu, J. & Mei, C. C. 2000 Do longshore bars shelter the shore? *J. Fluid Mech.* **404**, 251–268.

https://doi.org/10.1017/S0022112006004484 Published online by Cambridge University Press